Université de Montréal

α/β-hydrolase domain-6 and the development of high-fat diet-induced adipose tissue inflammation

Par

Clémence Schmitt

Université de Montréal, Programme de Biologie Moléculaire, Faculté de Médecine

Mémoire présenté en vue de l'obtention du grade de Maîtrise ès sciences

en Biologie Moléculaire, option Maladies complexes chez l'humain.

Avril, 2021

Université de Montréal

Unité académique : Programme de Biologie Moléculaire, Faculté de Médecine

---

Ce mémoire intitulé

α/β-hydrolase domain-6 and the development of high-fat diet-induced adipose tissue inflammation

Présenté par

Clémence Schmitt

A été évalué(e) par un jury composé des personnes suivantes :

Francis Rodier
Président-rapporteur

Marc Prentki
Directeur de recherche

Emile Levy
Membre du jury

Résumé

L'obésité est un facteur de risque important du diabète de type 2 et des maladies cardio-vasculaires. Durant le développement de l'obésité, le remodelage pathologique du tissu adipeux et l'inflammation locale contribuent à la mise en place d'une inflammation systémique, une accumulation de gras ectopique et une résistance à l'insuline. Les macrophages jouent un rôle important dans la régulation des voies signalétiques inflammatoires qui sont liées à leurs différents états d'activation. En effet, l'influence de diverses adipokines, cytokines et hormones ainsi que la disponibilité des nutriments vont induire leur polarisation en un phénotype soit pro-inflammatoire M1, soit anti-inflammatoire M2. De ce fait, comprendre les mécanismes et acteurs impliqués dans la polarisation des macrophages résidents du tissu adipeux vers un phénotype anti-inflammatoire M2 pourrait apporter une stratégie pour traiter les complications de l'obésité. La suppression de l'α/β-hydrolase domain-6 (ABHD6), une monoacylglycérol lipase, a démontré chez la souris des effets bénéfiques contre l'obésité, le diabète de type 2 et d'autres maladies inflammatoires. Cependant, le rôle précis de l'ABHD6 dans l'activation et la polarisation des macrophages en conditions inflammatoires, ainsi que les mécanismes sous-jacents, ne sont pas clairement définis. Le but de cette étude était d'investiguer : 1) le rôle immuno-métabolique de l'ABHD6 dans l'inflammation chronique du tissu adipeux induite par l'obésité chez la souris, et 2) le rôle régulateur de l'ABHD6 dans l'activation et la polarisation des macrophages dans des conditions inflammatoires aiguës induite par le lipopolysaccharide (LPS). En employant des approches pharmacologiques et génétiques, nous avons démontré que la délétion globale de l'ABHD6, chez les souris rendues obèses par une diète riche en gras, permet de maintenir un tissu adipeux sain au niveau immuno-métabolique. En effet, les souris ABHD6-KO nourries avec une diète riche en gras montrent une expression réduite de l'expression des marqueurs pro-inflammatoires (*Mcp1* and *Cd11c*), fibrotiques (*Col5a1*) et hypoxiques (*Hif1a*) dans tous leurs tissus adipeux (viscéral, sous-cutané et brun). Le nombre de macrophages pro-inflammatoires M1 est aussi diminué dans les tissus adipeux viscéral et brun des souris KO nourries à la diète grasse. De plus, la suppression de l'ABHD6 a changé la polarisation des macrophages d'un phénotype pro-inflammatoire M1 vers un phénotype anti-inflammatoire M2 dans des lignées cellulaires de

macrophages (RAW264.7 et J774A.1) et des macrophages péritonéaux primaires de souris traités avec le LPS.

Collectivement, nos résultats supportent la vision que l'ABHD6 a un rôle pro-inflammatoire dans induit par la diète riche en gras ou le LPS. Ces observations nous ont permis d'obtenir un aperçu du rôle de l'ABHD6 dans les voies immuno-métaboliques des tissus adipeux et suggèrent que l'ABHD6 pourrait être une cible thérapeutique intéressante pour contrer l'inflammation et les complications de l'obésité.

Mots-clés : ABHD6, obésité, tissu adipeux, adipokines, cytokines, monoacylglycérol, maladies métaboliques, inflammation, métabolisme.

Abstract

Obesity is a major risk factor for type 2 diabetes (T2D) and cardiovascular diseases. Pathologic adipose tissue (AT) remodeling and local inflammation contribute to systemic inflammation, ectopic fat accumulation and insulin resistance in obesity. Macrophages play an important role in inflammatory pathways, and these cells possess different activation states, M1 pro-inflammatory and M2 anti-inflammatory, influenced by adipokines, cytokines, hormones, and fuel availability. Thus, understanding the mechanisms and players involved in AT-resident macrophage polarization towards an anti-inflammatory M2 phenotype may provide a strategy to treat obesity complications. Suppression/deletion of the monoacylglycerol lipase α/β-hydrolase domain-6 (ABHD6) was previously shown to have beneficial effects against obesity, T2D, and other inflammatory disorders. However, it is not precisely known if ABHD6 plays any direct role in macrophage activation and polarization under inflammatory conditions, and if it does, the underlying mechanisms are yet to be defined. The aim of this study is to investigate: 1) the immunometabolic role of ABHD6 in obesity-induced chronic AT inflammation in mice, and 2) the regulatory role of ABHD6 in macrophage activation/polarization under conditions of acute lipopolysaccharide (LPS)-induced inflammation. Employing pharmacological and genetic approaches, we demonstrate that global ABHD6 deletion maintains AT immunometabolic health during diet-induced obesity in mice. High-fat-diet(HFD)-fed whole-body ABHD6-KO (HFD-ABHD6-KO) mice exhibit lower expression of pro-inflammatory (*Mcp1* and *Cd11c*), fibrosis (*Col5a1*) and hypoxia (*Hif1a*) markers in all fat depots. The pro-inflammatory M1-macrophages in the visceral and brown fat depots are also reduced in HFD-ABHD6-KO mice. Additionally, ABHD6 suppression switches LPS-induced macrophage polarization from an M1-like phenotype towards an anti-inflammatory M2 state in the macrophage cell lines (RAW264.7 and J774A.1) and in primary peritoneal macrophages.

Collectively, our results support the view that ABHD6 has a pro-inflammatory role under conditions of HFD- and LPS-induced inflammation. These findings provide an insight into the role

of ABHD6 in AT immunometabolic pathways in obesity, and suggest ABHD6 as a therapeutic target for inflammation and obesity-related complications.

Keywords : ABHD6, obesity, adipose tissue, adipokines, cytokines, monoacylglycerol, metabolic diseases, inflammation, metabolism.

Table des matières

Liste des tableaux

Liste des figures

Liste des sigles et abréviations

2-AG : 2-arachidonoylglycerol

ABHD6 : α/β-hydrolase domain-6

ACSL : acyl-CoA synthase

AGPAT : 1-acyl-*sn*-glycerol-3-phosphate acyltransferase

AKT : serine/threonine kinase 1

aP2 : adipocyte protein 2

Arg1 : arginase-1

ASO : antisense oligonucleotide

AT : adipose tissue

ATGL : adipose triglyceride lipase

ATM : adipose tissue macrophages

ATP : adenosine triphosphate

BAT : brown adipose tissue

BMI : body mass index

BMP : bone morphogenetic protein

BSA : bovine serum albumin

BW : body weight

C/EBP : CCAAT/enhancer-binding protein

CB : cannabinoid

CCR2 : chemokine receptor 2

CD : cluster of differentiation

CLS : crown-like structure

CNS : central nervous system

Col1a1 : Collagen type I alpha 1 chain

Col5a1 : Collagen type V alpha 1 chain

COX-2 : cyclooxygenase-2

CREB : cAMP response element-binding protein

DAG : diacylglycerol

DGAT : diacylglycerol acyltransferase

DMEM : Dulbecco's minimal essential media

EBF2 : early B-cell factor 2

ES : embryonic stem

FACoA : fatty acyl-Coenzyme A

FACS : fluorescence-activated cell sorting

FBS : fetal bovine serum

FFA : free fatty acid

FGF21 : fibroblast growth factor 21

FI : food intake

FOXO : forkhead box O

GIP : insulinotropic polypeptide

GL/FFA : glycerolipid/free fatty acid

GLP1 : glucagon-like peptide-1

GLUT4 : glucose transporter 4

GPAT : glycerophosphate acyltransferase

GPR : G protein-coupled receptor

Gro3P : glycerol-3-phosphate

gWAT : perigonadal white adipose tissue

HFD : high-fat-diet

HIF : hypoxia-inducible factor

HoxB6 : homeobox B6

HSL : hormone-sensitive lipase

IFN : interferon

IGFF1 : insulin-like growth factor 1

IL : interleukin

IL-4Rα : interleukin-4 receptor α

iNOS : inducible nitric oxide synthase

IRS : insulin receptor substrate

iWAT : inguinal white adipose tissue

KLF5 : Kruppel Like Factor 5

KO : knock-out

KRBH : Krebs-Ringer bicarbonate HEPES

LPA : lysophosphatidic acid

LPL : lipoprotein lipase

LPS : lipopolysaccharide

MAG : monoacylglycerol

MAGL : monoacylglycerol lipase

MAPK : mitogen-activated protein kinase

MCP-1 : monocyte chemotactic protein-1

Meox1 : mesenchyme homeobox 1

MHO : metabolically healthy obesity

Mrc1 : macrophage mannose receptor C-type 1

mTOR : mechanistic target of rapamycin

Myf5 : myogenic factor 5

NADFLD : non-alcoholic fatty liver disease

ND : normal diet

NF-κB : nuclear factor kappa-light-chain enhancer of activated B cells

NLRP3 : nucleotide oligomerization domain-like receptor family pyrin domain containing 3

NOS2 : nitric oxide synthase 2

PA : phosphatidic acid

PAP : phosphatidic acid phosphatase

Pax7 : paired box 7

PDG2-G : prostaglandin-D2-glycerol

PHARC : polyneuropathy, hearing loss, ataxia, retinitis pigmentosa and cataract

PI3K : phosphoinositide-3-kinase

PL : phospholipid

PM : peritoneal macrophage

PPAR : peroxisome proliferator activated receptor

PRDM16 : PR domain containing 16

Prx-1 : peroxiredoxin 1

RBC : red blood cell

RBP : retinol binding protein 4

RPMI : Roswell park memorial institute

SC : subcutaneous

SLE : systemic lupus erythematosus

SMAD4 : mothers against decapentaplegic homolog 4

SNS : sympathetic nervous system

STAT : signal transducer and activator of transcription 6

SVF : stromal vascular fraction

T2D : type 2 diabetes

TG : triglyceride

TLR : toll-like receptor

TNFα : tumor necrosis factor alpha

Treg : regulatory T cell

UCP1 : uncoupling protein 1

VC : visceral

VEGF : vascular endothelial growth factor

WAT : white adipose tissue

WB : whole-body

WHO : world health organization

WT : wild-type

ZPF423 : zinc finger protein 423

Contributions détaillées

Clémence Schmitt performed peritoneal macrophages isolation and polarization, macrophage cell lines culture, maintenance and polarization, and all the following experiments with primary and cell-line macrophages. She helped with tissue collections, SVF isolation, RNA extraction and quantifications. Clémence Schmitt wrote the thesis and participated in designing macrophage (primary and cell lines) experiments and analyzing of the results.

Pegah Poursharifi designed the project and supervised all the experiments. She performed tissue collections and SVF isolation, and adipose depots RNA extraction, mRNA and protein assessments. She performed the flow cytometry experiments and interpreted the results. She also helped with the writing of the thesis, data analysis and discussion of the study.

Isabelle Chenier participated in mice colony maintenance and genotyping, HFD feeding, body weight and food intake measurements, and tissue triglyceride content assay. Isabelle Chenier, Roxanne Lussier and Anfal Al-Mass helped with blood and tissue collections. Yat Hei Henry Leung helped with the macrophage cell lines maintenance.

Marc Prentki, Murthy Madiraju and Marie-Line Peyot supervised the project, designed the study, and helped with the interpretation of the data and the writing of the thesis.

À ma grand-mère Andrée, « sans toi rien ne sourit ».

Remerciements

I would like to thank my supervisor, Dr Marc Prentki, who saw potential in me since the first day we met. He is such a dedicated person, with an incredible passion for science and research. He encouraged me with fervor to believe in myself and to use my hidden qualities in order to grow into a curious and confident researcher.

I also want to thank Dr Murthy Madiraju, who has been an inspiring advisor. So many times, I have knocked at his door for advice. He has always guided the laboratory students to meditate, find their own solutions, and be scientifically curious. He finds himself accomplished when he contemplates his trainees rise and shine, and I have always admired his endless modesty.

I cannot thank enough Dr Pegah Poursharifi, my mentor. She has been such an inspiration for me of self-determination, curiosity and truthfulness. She has been extremely generous and patient with me at work, and she also has been deeply attentive to my personal well-being over the years. She has taught me so much, from the lab work to my own individuality.

Many thanks to Dr Marie-Line Peyot and Alix Zutter. They have been so committed to help me go through personal and work issues. They have both had my best interests at heart, and built a well-grounded environment for me to thrive.

I am so grateful for all the Prentki's lab members, students and technicians, who have helped, taught, and listened. We had great laughs and I have always felt so included from the beginning.

The MDRC and CRCHUM have built a great community that helped me grow as a scientist.

I also want to mention the program of Molecular Biology from the University of Montreal. They are so dedicated to their students and their career. A lot of professors have been eager for their students to succeed. I am so thankful for the scholarships they awarded me during my Master's.

And lastly, a special thanks to my family, which has always pushed me forward in everything that I was passionate about.

Chapter 1 - Introduction

1.1. Obesity

1.1.1. Definition and generalities

Overweight and obesity are defined by the World Health Organization (WHO) as “abnormal or excessive fat accumulation that may impair health” (1). This classification is based on body mass index (BMI), which is the weight in kilograms divided by the square of the height in meters (1). WHO guidelines define individuals with a BMI between 25 and 29.9 kg/m^2 as overweight and with a BMI greater than or equal to 30 kg/m^2 as obese. Although obesity is generally measured in terms of BMI, waist circumference and total adipose tissue (AT) mass have more impact on the development of metabolic disturbances (2). Obesity has been recognized as a major risk factor for many cardiometabolic diseases, such as type 2 diabetes (T2D), hypertriglyceridemia, hypercholesterolaemia, hypertension, non-alcoholic fatty liver disease, steatohepatitis and cardiovascular disease, and also cancer (2, 3). These comorbidities are often associated with the development of a low-grade chronic inflammation induced by maladaptive inflammatory response to a long-term positive energy balance (3). Indeed, some studies demonstrated the involvement of various immune cells, such as lymphocytes, neutrophils, and eosinophils, but mostly macrophages, in the regulation of metabolic homeostasis (4-7).

1.1.2. Epidemiology

During the last four decades, the worldwide prevalence of obesity nearly tripled and led to the associated rise in the healthcare costs (1). In 2016, more than 1,9 billion adults worldwide, i.e., 39% of the adult men and women, were overweight, of whom 650 million people were obese (13%). In the same year, the prevalence of obesity among Canadian adults was 29,4%. Moreover, it has been estimated that obesity and the overweight associated chronic diseases caused significant increase in the annual healthcare costs in Canada between 2000 and 2008 (from $3,9 billion to $4,6 billion). The economic burden rises to $7,1 billion when eighteen obesity-associated diseases are taken into account (8). Therefore, extensive research is essential to better

understand the cellular pathways involved in the pathophysiology of obesity, to identify the underlying molecular mechanisms, and to develop new therapeutic strategies.

1.2. Different adipose depots and their influence on the pathophysiology of obesity

AT plays an essential role in the regulation of energy homeostasis. In mammals, there are various types of AT, white, beige and brown, which are found in different locations. White adipose tissue (WAT) is dispersed all over the mammalian body into subcutaneous (SC) and visceral (VC) depots. Brown adipose tissue (BAT), however, is found in the interscapular space and along the cervical column in mice, but in human, it is mostly located in the supraclavicular space of the neck and next to the heart and cervical column (4). Each of these tissues contains different type of adipocytes, and has distinct metabolic features that proffer specific developmental and functional characteristics (4, 9). Also, the composition and distribution of ATs affect the development of obesity in different ways (**Figure 1**). For instance, the accumulation of VC WAT, under positive energy balance, is notably correlated with the development of insulin resistance and metabolic syndrome compared to SC WAT accumulation (2).

1.2.1. Role and localization

1.2.1.1. White adipose tissue

WAT represents a quarter of the body mass in lean individual, and is commonly categorized depending on its location. Thus, WAT serves as the principal fuel donor and depository. About one third of the cells composing the white fat depots are white adipocytes, surrounded by a rich microenvironment consisting of fibroblasts, immune cells, endothelial cells, beige adipocytes and preadipocytes, contributing to WAT function (2, 10). White adipocytes contain a large lipid droplet, pressing the nucleus to the periphery with very few mitochondria, whereas beige adipocytes contain several smaller lipid droplets and relatively more mitochondria to exert their thermogenic functions (see section 1.2.1.3 below).

Following the discovery of leptin, there has been great interest in understanding the endocrine function of AT (11). Studies have found that AT secretes various adipokines and cytokines that contribute to the regulation of the metabolic state systemically, and some of the adipokines/cytokines have been shown to be involved in low-grade inflammation (11, 12). This function of AT will be further discussed later in this thesis. White fat depots are often characterized as subcutaneous (under the skin) and visceral or intra-abdominal (10). SC WAT, by buffering excess lipids, could be protective in excess nutrition conditions. Whereas VC WAT is known to steadily conduct lipolysis and release free fatty acids (FFA) into the circulation, contributing greatly to insulin resistance and metabolic syndrome development (10) (**Figure 1**). It is important to mention that WAT is innervated by the sympathetic nervous system (SNS), which allows regulation of lipid storage and utilization (13).

1.2.1.2. Brown adipose tissue

Brown adipose depots represent less than 2% of total fat mass in lean human adults, and are localized in supraclavicular space of the neck and around the cervical column. In mice, the main brown depots lie in the interscapular space (4). Brown adipocytes are the main component of the BAT, and are designed to generate heat through the uncoupling of oxidative phosphorylation from electron transport by the mitochondrial uncoupling protein 1 (UCP1). It has been shown that BAT function is induced by cold and SNS activation. BAT is highly innervated by the SNS and sensory nerves, which are responsible to promote non-shivering thermogenesis and to regulate metabolism, mainly through UCP1 activation (14). BAT also supports excess glucose clearance from the circulation in response to insulin signalling, which helps to reduce metabolic pressure on the beta-cell to secrete high levels of insulin in response to glucose (**Figure 1**) (10). In contrast to WAT, BAT activity associates negatively with BMI and body fat (15).

1.2.1.3. Beige adipocytes

In animal models, it has been noticed that beige adipocytes exist within the white fat pads, mostly in SC WAT. Beige adipocytes can arise from beige preadipocytes that have a common lineage with white adipocytes, or emerge by the trans-differentiation of mature white adipocytes into mature beige adipocytes (4, 11). Although white and beige adipocytes have a shared lineage, beige

preadipocytes, like brown precursors, require a specific EBF2 (early B-cell factor 2) transcription factor to drive beige adipogenesis, while white adipocyte commitment factor ZPF423 (zinc finger protein 423) inhibits EBF2 to induce white adipocyte adipogenesis (see section 1.2.3. below) (16, 17). Additionally, the differentiation of beige preadipocytes into mature adipocytes is stimulated by various signals, such as cold, exercise or adrenergic stimulation, and gives those cells brown adipocyte-like functions (3, 18). Indeed, these adipocyte subtypes have higher number of mitochondria and UCP1 expression compared to the white adipocytes, and display triglyceride-lowering and thermogenesis capabilities. However, they exhibit a distinctive expression of inflammation- and metabolism-involved genes compared to brown and white adipocytes (10, 11). Studies showed that obese individuals have less beige and brown AT than lean individuals and that defective differentiation into beige adipose is linked to weight gain. Thus, beige adipocytes appear to play an important role in metabolism and energy expenditure (4).

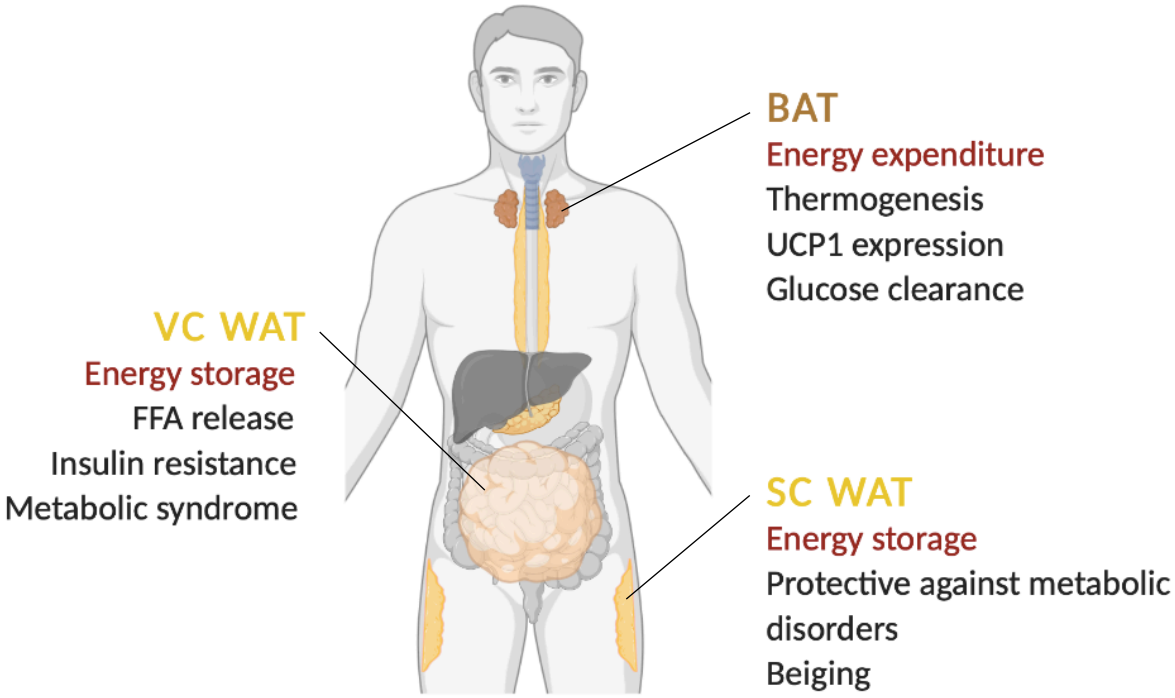

Figure 1. Human adipose depots.

BAT likely plays a considerable role in energy expenditure and thermogenesis in humans. WAT depots are involved in energy storage. Under obese conditions, VC WAT expansion contributes

to insulin resistance and metabolic syndrome, while SC WAT expansion is protective by reducing ectopic lipid accumulation (18, 19).

1.2.2. Adipose tissue cell composition determines healthy metabolic states

Even though adipocytes are the main constituents of the AT, it also contains a large panel of other cell types, including immune cells, fibroblasts, endothelial cells, mesenchymal stem cells, and preadipocytes. Fractionation of fat depots, *ex vivo* gives rise to two separate cellular fractions, the floating mature adipocytes and the heterogenous cell pellet, called stromal vascular fraction (SVF) (2, 4). The SVF consists of immune cells that are essential to maintain immune homeostasis, and fibroblasts, endothelial cells, mesenchymal stem cells and preadipocytes, which co-operate to preserve AT function and structure.

1.2.2.1. Inter-/intra-depot adipocyte heterogeneity influences metabolic functions of adipose tissue

Functional and cellular differences exist between different adipocytes within a fat depot and from different depots. Unique gene expression profile of preadipocytes isolated from SC depot, together with their distinct adipokine/cytokine secretion and associated signaling cascades, contribute to higher rates of *ex vivo* proliferation/differentiation and lipid accumulation in this depot (18). However, VC preadipocytes exhibit less *ex vivo* differentiation capacity, while mature VC adipocytes display higher rate of lipolysis and are more prone to hypoxia and apoptosis, in comparison to the SC adipocytes (18, 19). Consistently, compared to VC, SC fat secretes more adiponectin, which has been shown to improve insulin sensitivity and lipid clearance, demonstrating its anti-inflammatory abilities. Conversely, VC fat secretes higher levels of resistin and retinol binding protein 4 (RBP4), which are associated with insulin resistance and T2D (19). The recent discovery of functionally and developmentally different adipocyte progenitors explains the presence of various types of mature adipocytes that display distinct location-specific metabolic functions (18, 19).

1.2.2.2. Adipose tissue macrophages sustain metabolic homeostasis

1.2.2.2.1. Macrophage activation states

In the AT from lean individuals, macrophages represent approximately 10% of the total immune cells (20). Macrophages are a diversified class of hematopoietic cells that act as the sentinels of the innate immune system. They are present in many tissues, tracking infections or cellular damage by sensing the inflammatory signals within their microenvironment. Depending on the external stimulus, macrophages exhibit different activation states: the classically activated M1 and the alternatively activated M2 macrophages (**Figure 2**) (21). The classical activation state, i.e., the polarization of macrophages into M1 macrophages, is stimulated by the presence of lipopolysaccharide (LPS), Toll-like receptor (TLR) ligands or cytokines, like interferon-γ (IFN-γ) or tumor necrosis factor alpha (TNFα). M1 macrophages display high phagocytic and bactericidal characteristics and secrete pro-inflammatory cytokines (21). Several pathways are involved in the secretion process, such as the activation and the nuclear translocation of the nuclear factor kappa-light-chain enhancer of activated B cells (NF-κB) (21). Conversely, the alternative activation of macrophages to M2 state takes place in response to parasitic infections and the presence of interleukins (IL)-4 and -13, favoring antiparasitic and tissue repair characteristics of the macrophages, which secrete anti-inflammatory cytokines. One of the main anti-inflammatory pathways activated in the M2 macrophages is the signal transducer and activator of transcription 6 (STAT6) (4, 7, 22). Macrophage polarization has pathological role, shown by the involvement of M1 macrophages in inflammatory diseases, such as atherosclerosis and inflammatory bowel diseases (22). In addition, it has been shown that deletion of STAT6, IL-4, IL-13 and their receptor, IL-4 receptor α (IL-4Rα) in mice, leads to compromised function of M2 macrophages and reduced expression of UCP1 in beige and brown adipocytes and WAT browning, in association with impaired maintenance of core body temperature (4).

More recently, studies have demonstrated that macrophages can adopt more than two activation states within the AT, depending on the fat pad location and the nutritional status, and are recognized by the expression of surface markers (6). For example, the cluster of differentiation molecule 11c (CD11c) is considered as a general M1-like marker and most of the AT infiltrated

monocytes will express CD11c in all the fat depots during obesity and has been linked with insulin resistance (2, 7). Both M1 and M2 macrophages express F4/80 and CD11b markers (7, 10). However, few other studies argue that F4/80 marker is more expressed in M1 macrophages, and that CD11b is not specific to macrophages but present in other immune cells as well (23, 24). Other macrophage markers include NOS2 (Nitric Oxide Synthase 2) and TNFα for M1, and Arg1 (arginase-1), CD206 and CD301 for M2 (20).

1.2.2.2.2. Macrophage activation state influences adipose tissue metabolic homeostasis

Various studies have reported that AT-resident M2 macrophages counteract with the development of diet-induced obesity, T2D and meta-inflammation (low-grade chronic inflammation throughout the body induced by long-term overnutrition and obesity) (6, 25). Indeed, AT M2 macrophages were found to be involved in the regulation of metabolic functions, such as adipocyte insulin sensitivity, through the activation of peroxisome proliferator activated receptor-γ (PPARγ) signaling pathway (6, 25). It has also been shown, in the context of obesity, that AT-resident macrophages could switch from M2-like phenotype to M1-like phenotype with the activation of the NLRP3 (nucleotide oligomerization domain-like receptor family pyrin domain containing 3) inflammasome signaling pathway (25). Also, M1 macrophages are able to switch back to M2-like phenotype, for example when high-fat-diet(HFD)-fed obese mice are given chow diet and upon insulin sensitivity amelioration (7). Therefore, the maintenance of balance in AT immune responses is crucial to sustain metabolic homeostasis within the AT microenvironment (6).

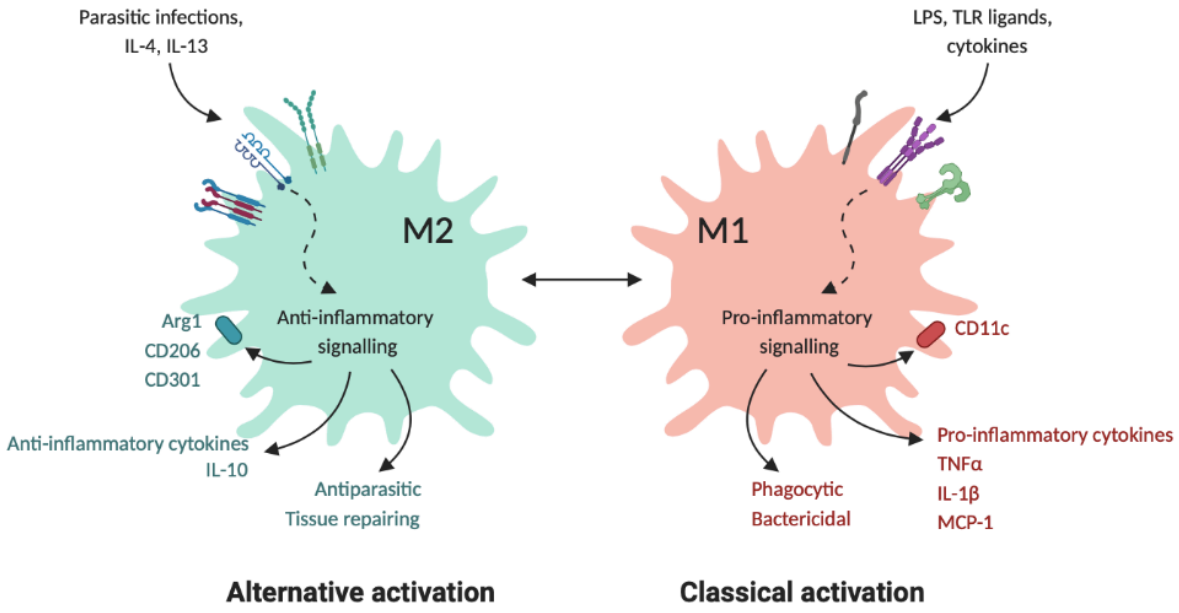

Figure 2. Macrophage activation state characteristics.

Pro-inflammatory signals promote the classical macrophage activation through the activation of transcription factors such as NF-κB, STAT1, or STAT3, which induce the secretion of pro-inflammatory cytokines and the expression of markers like NOS2. M1 macrophages then display phagocytic and bactericidal characteristics. Anti-inflammatory signals promote the alternative activation (M2) through the activation of transcription factors such as STAT6 or PPARγ, which induce the secretion of anti-inflammatory cytokines and the expression of markers like Arg1 (21). MCP-1, monocyte chemotactic protein-1.

1.2.2.3. Other cells in the adipose tissue

In addition to the macrophages, other immune cells, such as T and B lymphocytes, and dendritic cells reside in the VC WAT of obese individuals and are linked to obesity-induced inflammation pathophysiology (20). Lymphocytes represent 5 to 10% of the immune cells in WAT depots and are recognized by surface markers, like CD8+ or CD4+ for T cells or CD19+ for B cells (26). The proportion of T cells and B cells increases in the context of obesity, whereas regulatory T cells (Treg) are reduced. Indeed, Tregs are known to be involved in the regulation of immune and glucose homeostasis in the adipose tissue (20). In the same way, B cells display a greater pro-

inflammatory phenotype by secreting IFN-γ or IL-6 in diet-induced obese mice, while regulatory B cells have a protective effect on inflammation and insulin sensitivity (20, 23). In addition, AT-resident endothelial cells have important roles in the maintenance of AT health, by supplying nutrients, hormones, oxygen and growth factors through the blood vessels. In return, adipocytes secrete adipokines and angiogenic modulators to regulate angiogenesis (27). Fibroblasts have a more structural function and help adipocytes to preserve the extra-cellular matrix, which is composed of several proteins and glycoproteins involved in the tissue structure (27). These fibroblasts are also implicated in sustaining the pool of preadipocytes (18).

1.2.3. Adipogenesis and angiogenesis

1.2.3.1. Adipocyte lineage

Originally, adipocyte lineage was deduced on the basis of the expression of mesoderm-specific genes Myf5 (Myogenic Factor 5) and Pax7 (Paired Box 7). Recent investigations showed that the lineage is more complicated. Meox1 (Mesenchyme Homeobox 1), Pax3/7 and Myf5 expression actually lead to brown adipocytes and skeletal muscle, as well as retroperitoneal and interscapular white adipocytes. Progenitors marked with HoxB6 (Homeobox B6) give rise to other WAT depots, while those expressing Prx-1 (Peroxiredoxin 1) generate only SC adipocytes (18). Other studies demonstrated a vascular origin of the adipocyte precursors using different preadipocyte markers (18).

1.2.3.2. Adipocyte differentiation contributes to metabolic health

Adipocytes respond to systemic stimuli by either storing lipids as triglycerides or depleting their stocks of nutrients. During fasting or exercise, adipocytes deplete their triglyceride stock via lipolysis to supply energy as fatty acids (10). In conditions of excess calorie intake, metabolic health depends on the capacity of AT to expand via two processes. Initially, adipogenesis can occur by hyperplasia, which is the differentiation of progenitors to create new adipocytes. Secondly, differentiated adipocytes can increase their size (hypertrophy) by storing lipids in the form of lipid droplets. However, while adipocyte hyperplasia has been shown to counteract obesity-related metabolic impairments, adipose hypertrophy associates with insulin resistance and inflammation (10, 11). In fact, hypertrophy induces mechanical and hypoxic stresses on

adipocytes, leading to AT inflammation in the long run. Those hypertrophic adipocytes also display phenotypic characteristics, with an increased secretion of pro-inflammatory adipokines and lipolysis, that correlate with reduced anti-inflammatory cytokines and adipokines secretion (**Figure 3**). Consequently, AT metabolic health requires the coordination between the different adipose resident cell types to prevent hypoxia by driving AT remodelling and angiogenesis (3, 27).

Mature adipocytes appear to display distinct metabolic functions depending on their depot localization. Thus enhanced differentiation of brown and beige adipocytes allows amplification of their functions, such as thermogenesis, insulin sensitivity, glucose tolerance and lipid oxidation. Similarly, SC WAT expansion allows a greater lipid storage and oxidation, and anti-inflammatory function to prevent metabolic disturbances and ectopic fat accumulation. Conversely, in the obesity context, VC WAT differentiation has less beneficial role, as it is linked to insulin resistance, cardiometabolic diseases and obesity-induced inflammation (28).

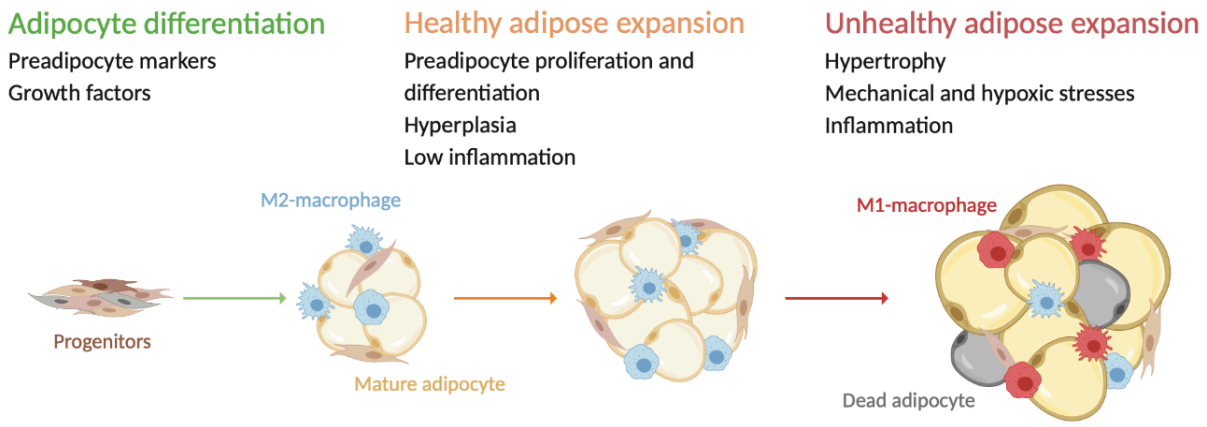

Figure 3. Metabolic health depends on healthy expansion of adipose tissue.

From left to right, preadipocytes differentiate into mature adipocytes depending on adipogenic factors. Under healthy conditions, AT sustains its differentiation capacity, resulting in insulin sensitivity and low levels of inflammation. When AT loses its differentiation capacity, adipocyte hypertrophy leads to inflammation, insulin resistance, hypoxia, metabolic stresses and tissue damage. This transition from healthy to unhealthy expansion induces the recruitment and the activation of M1 macrophages (18).

1.2.3.3. Adipogenesis depends on lineage specificity and PPARγ activation

Adipocyte differentiation causes changes in cell morphology, gene expression and sensitivity to hormones (29). Classically, adipogenesis occurs in two consecutive steps: the commitment of a mesenchymal precursor cell into a preadipocyte, followed by the differentiation of the preadipocyte into a mature adipocyte (**Figure 4**) (11). The adipogenic commitment consists of a process by which early adipogenic factors promote the precursor cells to acquire adipocyte lineage-specific markers and thereby lose their ability to differentiate into mesenchymal cell types, such as osteoblasts, myoblasts and chondroblasts. During this step, the fibroblast-like shaped precursor cell acquires the adipocyte morphology, except for the lipid droplets that arise during differentiation (30). The nuclear receptor PPARγ is known as the master regulator of adipogenesis (11). Its activation in the committed preadipocytes occurs via the stimulation of SMAD4 (mothers against decapentaplegic homolog 4) by bone morphogenetic protein (BMP)2 and BMP4 pathway (11). Moreover, other transcription factors and master regulators are involved at different steps of adipocyte commitment. For example, ZFP467 transcription factor and KLF5 (Kruppel like factor 5) can stimulate adipogenesis by stimulating the co-activator CCAAT/enhancer-binding protein-α (C/EBPα) and C/EBPβ, respectively (11). Conversely, GATA2 and 3 inhibit adipogenesis by restricting PPARγ transcription (11). In fact, PPARγ also activates C/EBPα and both act in synergy to drive adipocyte differentiation. In response, C/EBPα and β trigger the transcription of mature adipocyte genes, encoding adipocyte protein 2 (aP2), adiponectin and the insulin receptor (11). It is important to note that PPARγ, as well as PR domain containing 16 (PRDM16), are indispensable for activating BAT differentiation and thermogenesis program, and SC WAT browning (15). The complexity of adipogenesis resides in the heterogenicity of lineage markers and the large panel of signalling ligands and hormones that are able to modulate intracellular cascades, that are implicated in this process.

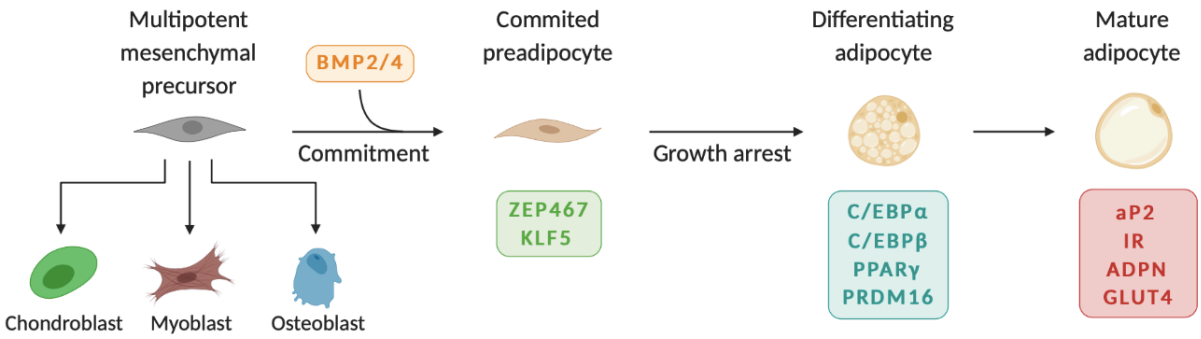

Figure 4. Molecular mechanism of adipogenesis from precursor to mature adipocyte.

The commitment of a progenitor cell depends on lineage-specific markers and adipogenic factor activation. Other transcription factors are needed for differentiation into mature adipocyte and they act in synergy. The mature adipocyte acquires specific markers and expresses specific proteins that determine its function (11). ADPN, adiponectin; IR, insulin receptor.

1.2.3.4. Signalling via hormones and ligands modulates adipogenesis

In vitro, adipogenic cells need a special hormonal cocktail to differentiate into mature adipocytes (11). Insulin is the main component of this cocktail and allows these cells to differentiate even without additional hormones. By binding to its receptor, insulin activates insulin receptor substrates (IRSs), PI3K (phosphoinositide-3-kinase) and AKT (serine/threonine kinase 1) kinases, leading to the activation of several downstream proteins such as CREB (cAMP response element-binding protein), mTOR (mechanistic target of rapamycin) and FOXO (forkhead box O) (11). Insulin also binds with lower affinity to insulin-like growth factor 1 (IGF1) receptor, present on many cells including preadipocytes. However, inhibition of any one of the signalling components of this pathway represses adipocyte differentiation *in vitro* (11). Conversely, elevated blood glucose and insulin in obesity context could be involved in AT hyperplasia (11).

The *in vitro* adipogenic hormonal cocktail also contains dexamethasone, which is a synthetic glucocorticoid, that is needed for terminal differentiation. Glucocorticoid pathway amplifies insulin signalling and C/EBPs in preadipocytes. The glucocorticoid receptor is ubiquitous and is involved in the utilization of nutrients and prevention of inflammation (11). Further, chronically

elevated glucocorticoid plasma level in obesity has been linked to the development of metabolic syndrome, insulin resistance, hyperglycemia and dyslipidemia (31).

Other ligands have been found to modulate adipogenesis, such as WNTs and Hedgehog ligands (11). WNT inhibits adipogenesis by preventing PPARγ and C/EBPα activation in preadipocytes, whereas Hedgehog ligands impede insulin and BMP signalling (11).

1.2.3.5. Angiogenesis prevents hypoxia during adipogenesis

In the AT environment, the vasculature is essential to maintain nutrients, oxygen, hormones and growth factors levels for adipogenesis, and thereby to remove metabolic wastes (27). Due to the increased requirement for oxygen during AT growth, local hypoxia promotes adipocytes to induce angiogenesis and glycolysis through hypoxia-inducible factor (HIF) alpha (27). The two subunits of HIFα have opposing roles, as HIF-1α has been shown to be pro-angiogenic, -fibrotic and -inflammatory, whereas HIF-1β prevents obesity-induced inflammation (27, 32). HIF-1α is also upregulated in expanding VC adipose due to chronic hypoxia during obesity (27). AT angiogenesis can occur through two mechanisms: sprouting and splitting. Sprouting angiogenesis consists of the formation of new vessels by endothelial cells migrating toward chemotactic and pro-angiogenic signals from adipocytes, like VEGF (vascular endothelial growth factor) secretion. Splitting angiogenesis occurs because of the division of a vessel in two due to the contraction of myofibroblast during wound healing. Sprouting angiogenesis could be induced in the early stages of obesity and be replaced by splitting angiogenesis in a chronic state, as VEGF signalling decreases and myofibroblast activation increases (27).

1.3. Role of adipose tissue in energy homeostasis and metabolism

Adipocytes play a central role in regulating systemic energy homeostasis through their ability to store and release fatty acids, depending on the energy status. AT metabolism and thermogenesis are tightly regulated by central nervous system (CNS) and autocrine/paracrine/endocrine factors, such as hormones, adipokines and cytokines (10, 11).

1.3.1. The adipose tissue as an endocrine tissue

In addition to its classical functions of energy storage and distribution, AT also acts as an important endocrine organ that produces many bioactive molecules called adipokines. Adipokines can be hormones, cytokines, growth factors or angiogenic factors, and can operate in an autocrine, paracrine or endocrine way. Adipokine secretion depends on the energy status and varies among different fat depots, to regulate AT metabolism (33). Besides the adipocytes, immune cells, endothelial cells, preadipocytes and fibroblasts also contribute greatly to its secretory activity (10, 33).

1.3.1.1. The adipokines are regulating the systemic energy homeostasis and inflammation

Adipokines are AT-secreted hormones/cytokines that have various effects throughout the body. For example, they are responsible for regulating lipogenesis, glucose homeostasis, energy expenditure, insulin signaling, inflammation and energy expenditure in metabolically active organs, but also physiological functions like appetite and satiety (10, 34). The main adipokines released by AT into the circulation are leptin, adiponectin and resistin and are discussed below (**Table 1**. (10). Other cytokines have various paracrine and autocrine effects within the microenvironment of AT and are further discussed below (10).

Leptin is a pro-inflammatory cytokine, expressed predominantly by SC WAT, and has important roles in the regulation of appetite, satiety and energy expenditure (34, 35). Leptin blood level is proportional to the total fat mass. During periods of feeding, leptin exerts paracrine effects on the afferent nerve fibers, innervating the AT, via binding to the leptin receptor. The signaling cascade triggered in the afferent fibers sends signals to the brain that fat storage in the AT is increasing, and this results in a feedback signal from hypothalamus to limit food intake and triglyceride accumulation (36). It also has an endocrine effect directly on the hypothalamus, through its receptor, inducing satiety, energy expenditure, heat loss, and also hepatic gluconeogenesis (18). During fasting, a decline in leptin level acts as a homeostatic signal to inform the CNS to promote feeding by increasing appetite and decreasing energy expenditure (4, 18, 34-37). This hypothesis was first supported by a study showing that leptin injection during

starvation prevented this fasting induced signal, and abrogated appetite increase and energy expenditure suppression (38). However, under pathophysiological conditions such as metabolic syndrome and obesity, leptin function and signaling may be compromised (**Table 1**. due to "leptin resistance" (34). Of note, leptin receptor is also found on immune cells and leptin signalling promotes various effects in these cells such as chemotaxis and pro-inflammatory cytokine release (39). In addition to leptin, resistin is another pro-inflammatory cytokine, which is only secreted by AT-resident macrophages and monocytes in humans, and increases with obesity (35). Resistin plays a role in different metabolic diseases and cell types and is mainly known to worsen insulin resistance and inflammation (**Table 1**. (35). Lastly, in contrast to leptin and resistin, adiponectin is an anti-inflammatory and systemic insulin-sensitizing cytokine. Adiponectin is the most abundant serum adipokine produced mainly by SC WAT, and in contrast to leptin, its levels are inversely proportional to total fat mass (4, 18, 35). Adiponectin acts on many tissues by binding to either of its two receptors, AdipoR1 or AdipoR2, depending on the cell type. Adiponectin exhibits protective effects on various biological processes, including hepatic gluconeogenesis, hepatic and muscle fatty acid oxidation, and AT glucose uptake and inflammation (**Table 1**. Adiponectin also inhibits proliferation and phagocytosis, and promotes apoptosis, M2 polarization on macrophages and anti-inflammatory cytokines production (18, 35).

Adipokines	Healthy AT	Hypertrophic AT	Effects
Leptin	↓	↑	↑ energy expenditure, satiety, hepatic glucogenesis ↓ appetite, heat loss, insulin secretion and resistance
Adiponectin	↑	↓	↑ hepatic and muscle FA oxidation, appetite, glucose uptake, insulin sensitivity ↓ hepatic glucogenesis, energy expenditure, inflammation
Resistin	↓	↑	↑ insulin resistance, inflammation

Table 1. The adipokines secreted by the adipose tissue in healthy and unhealthy conditions, and their endocrine effects.

Leptin is a pro-inflammatory cytokine that is upregulated in overfeeding conditions. Its secretion has a protective effect at first but during obesity development, a leptin resistance appears and leptin fails to exert its functions. Adiponectin is an anti-inflammatory cytokine, which is downregulated in obese condition. Its function to reduce inflammation and increase insulin sensitivity become less efficient as AT is growing. Resistin is a pro-inflammatory cytokine that is upregulated in hypertrophic AT and has detrimental functions (35).

1.3.1.2. Secretion of pro-inflammatory cytokines in the adipose tissue environment amplifies the inflammatory response to overnutrition

Beyond the three adipokines described above, AT secretes many other proteins, growth factors and cytokines having paracrine and autocrine effects within the AT microenvironment. The cytokines are often classified in two groups: the pro-inflammatory cytokines and the anti-inflammatory cytokines.

RBP4 is a pro-inflammatory cytokine produced by adipocytes, hepatocytes and macrophages, and is known to be a systemic transporter of vitamin A, and has been linked to obesity, inflammation, and insulin resistance (34). RBP4 exerts pro-inflammatory effects by activating antigen presenting cells and this function of RBP4 appears to be independent of its ability to bind with retinoids (40). During the initial stages of the obesity-induced inflammation development, hypertrophic adipocytes, located in VC WAT secrete an important chemokine, the monocyte chemotactic protein-1 (MCP1), which attracts circulating monocytes into the AT. MCP1 chemotactic gradient attracts monocytes and macrophages within the AT, and binds to the chemokine receptor 2 (CCR2) on macrophages (7). In response, macrophages secrete more MCP1, amplifying the recruitment of additional immune cells in the AT (10). Furthermore, M1 macrophages activated by pro-inflammatory signals secrete many pro-inflammatory cytokines, such as IL-1β, TNFα, IFN-γ and IL-6 (4). TNFα, for example, causes insulin resistance by activating serine kinases, which act on IRS-1 to attenuate insulin signaling. IL-1β is the product of inflammasome activation and is involved in the impairment of glucose tolerance and insulin sensitivity (7). The role of IL-6 is controversial and depends on the tissue environment or the type of cells. It has been

demonstrated to negatively affect insulin sensitivity in liver and AT, but positively in skeletal muscle (7). In summary, this feedback loop between adipocytes and macrophages leads to a local amplification of the pro-inflammatory response to overnutrition.

Further, VC WAT is generally demonstrated to secrete higher levels of pro-inflammatory cytokines such as MCP1, IL-6 and RBP4 in comparison to the SC WAT. Therefore, obesity-associated inflammation has been suggested to positively correlate specifically with VC expansion (19). Also, during obesity development, M2 macrophages are prone to switch to a M1-like phenotype, in part through obesity-induced RBP4 upregulation in WAT. In these macrophages IL-10 expression is reduced and pro-inflammatory cytokines expression is upregulated (4). In conclusion, the inflammatory crosstalk among different AT-resident cells plays a prominent role not only in the inflammation state of adipose microenvironment, but also in the progression of obesity-related systemic inflammation in the long run.

1.3.1.3. Secretion of anti-inflammatory cytokines helps maintaining an healthy adipose tissue environment during overnutrition

In addition to the pro-inflammatory cytokines, anti-inflammatory cytokines are secreted within the AT to favor metabolic health and protect itself against inflammation, principally by promoting M2-macrophage activation. The main anti-inflammatory cytokines involved in the alternative macrophage polarization are IL-4 and IL-13, which are produced in the AT by all types of adipocytes, eosinophils and type-2 innate lymphoid cells in lean/healthy conditions (39, 41). Following the macrophage polarization by IL-4/IL-13, the newly activated M2 macrophages inhibit IL-1β pathway by secreting IL-1 receptor antagonist. These M2 macrophages also produce another anti-inflammatory cytokine, IL-10, that antagonizes the effects of pro-inflammatory cytokine, including TNFα mediated downregulation of glucose transporter 4 (GLUT4). IL-10 also acts on adipocytes by decreasing MCP1 expression (4, 7, 21). Apart from IL-10, IGF-1, Arg-1 and VEGF-A are other known M2 macrophage-derived mediators, whose anti-inflammatory action resides in promoting tissue remodeling/repair and angiogenesis.

1.3.1.4. Regulatory effects of adipokines secreted from brown adipocytes

As BAT and WAT have different function and morphology, the adipokines from BAT, also called batokines, are secreted in response to distinct stimuli than the WAT adipokines, and have specific functions. In response to cold or norepinephrine signaling through the β3-adrenergic pathway, fibroblast growth factor 21 (FGF21) is secreted by BAT and beige WAT in mice (42). FGF21 is involved in the regulation of glucose and lipid metabolism in WAT and liver, and in BAT, FGF21 induces glucose uptake and oxidation, lipolysis and inhibits lipogenesis. FGF21 also promotes thermogenesis in BAT and beige adipose by stimulating UCP1 expression (42). Another factor promoting thermogenesis in BAT is VEGF-A. This adipokine is known to be involved in angiogenesis in both BAT and WAT, but specific overexpression of VEGF-A in brown adipocytes also induces UCP1 expression (42, 43). In addition, several studies documented the secretion of IL-6 from BAT through β3-adrenergic stimulation (44-47). But IL-6 involvement in BAT remains elusive (48). Lastly, in brown and beige adipocytes, cold exposure induces secretion of prostaglandins, such as prostaglandin I_2 and E_2, and the expression of lipocalins and prostaglandin D synthase, which are involved in the regulation of WAT browning and BAT function (42).

1.3.2. Adipose tissue metabolic adaptation in response to overnutrition

1.3.2.1. The physiologic changes in the adipose tissue microenvironment during the development of obesity

In positive energy balance conditions, the expansion of VC WAT has been found to be linked with the development of cardiometabolic disease, whereas SC WAT expansion seems to be protective (49). Thus, the mechanisms of WAT expansion in obesity are of interest to better understand the obesity-associated pathologies. As mentioned previously, two physiological processes by which adipose depots expand have been identified (11). Adipocyte hyperplasia occurs during the initial stages of obesity development and defined by *de novo* differentiation of progenitors into new mature adipocytes. During obesity advancement, adipocytes lose their capacity to differentiate and adapt to hypertrophic growth by expanding the existing lipid droplets. However, long-term positive energy balance, leads to AT hypoxia, cell death, inflammation, fibrosis, and finally lipid spill-over into other tissues (ectopic fat accumulation) (50-52). First, VEGF-A expression decreases

in overfeeding conditions impairing angiogenesis. Then, hypoxic conditions induce HIF-1α, to correct detrimental repercussions of hypertrophic adipocyte expansion by increasing angiogenesis and fibrosis (23, 27, 51). However, the chronic hypoxia engenders adipocyte death, secretion of pro-inflammatory cytokines and adipokines (which appears to be determined by the location of fat depot and the adipocyte subtype involved (11, 12)) and macrophage infiltration (23, 51). All of these events trigger the crown-like structure (CLS) formation, which is an arrangement of M1 macrophages around the apoptotic adipocytes to clean the adipocyte cellular content released in the microenvironment (2, 10, 27, 51). Mechanistically, three major pathways are involved. First, FFA, among other signals, released from the dead adipocytes can activate TLRs, which in return activate NF-κB and mitogen-activated protein kinase (MAPK) pathways leading to insulin signalling inhibition and pro-inflammatory cytokine production by macrophages and adipocytes (3, 53). Besides, dead adipocyte signals also induce macrophages to produce reactive oxygen species (ROS) that activate NLRP3 inflammasome leading to pro-inflammatory cytokines secretion, especially IL-1β (53). Even though macrophage infiltration in BAT has also been demonstrated, BAT seems to be more resistant to it and less sensitive to inflammation in diet-induced obese mice (54-56). However, macrophage infiltration, cell death and CLS formation in BAT lead to the whitening of brown adipocytes, which means that they form an unique large lipid droplet and lose mitochondria (56). Furthermore, the term metabolically healthy obesity (MHO) has been proposed to categorize the patients with obesity who are exceptionally metabolically healthy, exhibiting hyperplastic WAT expansion, less inflammation, and better insulin sensitivity. Thus, it was hypothesized that adipocytes in elevated number rather than increased size could be protective against obesity-associated metabolic diseases (50, 52).

1.3.2.2. Low-grade inflammation and organs/tissues cross-talk during obesity pathogenesis

As obesity progresses, all the events described in the previous section lead to development of obesity-induced low-grade chronic inflammation, also known as meta-inflammation. The AT pro-inflammatory immune response progressively impedes adipocytes insulin sensitivity and signalling, as well as the metabolic homeostasis and lipid storage. Then, the oxidative stress becomes lethal to both macrophages and adipocytes, and AT macrophage infiltration increases

to clear out the dead cells in order to allow tissue repairs (6, 27). Moreover, impaired metabolic and inflammation response under obese condition also occurs in other organs and tissues, and has been associated with the development of cardiometabolic and immune diseases (12). Liver has its own resident macrophages, the Kupffer cells, that are also able to change their activation state and display a pro-inflammatory profile in response to overnutrition (7). Through the progression of obesity, even though the number of Kupffer cells seems to be stable, circulating monocytes are infiltrating the tissue (57). The hepatic pro-inflammatory macrophages are then able to stimulate hepatocyte immune response leading to non-alcoholic fatty liver disease (NAFLD) and hepatic insulin resistance (7). Intramuscular fat of skeletal muscle can be infiltrated by macrophages that display M1-like characteristics and participate to muscle insulin resistance (6, 7, 58). A similar pro-inflammatory macrophage infiltration process is also seen in pancreatic islets, and leads to reduced insulin secretion, β-cell dysfunction and death (6, 59). Besides, CNS resident macrophages, known as the microglia, are also activated toward a pro-inflammatory profile during obesity progression, leading to leptin resistance in the hypothalamus (7, 60). Lastly, the gut microbiome inflammatory response has been associated to insulin resistance and glucose intolerance during obesity pathogenesis (7). Cytokines, adipokines and FFA secretion locally and through the circulation lead to the systemic low-grade inflammation and insulin resistance, and AT is at the center of this crosstalk between organs and tissues.

1.3.3. Adipose tissue is a central player in the regulation of lipid metabolism

WAT principal function is to serve as a fuel donor and depository for the whole body, and in order to fulfill its physiological roles, it can sense and respond to several metabolic signals (11). During exercise or negative energy balance, the decreasing glycemia induces glucagon or noradrenaline secretion, which stimulates adipocyte lipases, like hormone-sensitive lipase (HSL), adipose triglyceride lipase (ATGL) and monoacylglycerol lipase (MAGL) (11, 61). Those lipases are part of the glycerolipid/free fatty acid (GL/FFA) cycle, which produces many signalling molecules that are essential to maintain cellular metabolic homeostasis (61). Two important molecules produced during lipolysis are FFA and glycerol, which leave the lipid droplets to travel through the circulation to other organs. When the energy balance is positive, the increasing glycemia induces insulin secretion from the pancreas which inhibits HSL and ATGL in the adipocytes, in order to

stimulate glucose uptake and *de novo* lipogenesis to store the excess nutrients in the lipid droplets (11). However, during the development of obesity, the adipocytes fail to respond to those signals and this leads to elevated plasma glucose and lipids, high pro-inflammatory cytokines secretion, fibrosis and adipocytes cell death (11).

1.3.3.1. Lipid metabolism

Lipids are essential for several biological functions, ranging from cellular structure and energy storage to cell signaling. These multifunctional molecules are classified based on their structure into a broad range of lipids, such as fatty acids, phospholipids, sterols, sphingolipids and many more. Lipid metabolism involves uptake, lipogenesis, storage, and degradation of lipids to satisfy the metabolic needs of the cells. These processes are tightly regulated and are governed by many enzymes that constitute a number of specific pathways participate in the biosynthesis and degradation of lipids (61, 62). Consequently, any disturbances in lipid metabolism can lead to the pathogenesis of several metabolic diseases, such as obesity, T2D, metabolic syndrome, NAFLD, inflammation, and cancer (61).

During the digestion, fats from the alimentation are digested and then absorbed by the epithelial cells of the intestine to be incorporated as triglycerides (TGs) in the chylomicrons, which are released into the circulation (62). The lipoprotein lipase (LPL) at the surface of AT capillaries hydrolyzes lipoprotein-incorporated TGs into 2,3-diacylglycerol (DAG), then 2-monoacylglycerol (MAG) and lastly into FFA and glycerol (62). Circulating FFA will be transferred to the adipocytes by different FA transporters, such as CD36 (63, 64). When needed, the imported FAs will be stored as neutral lipids (mainly TGs) in the lipid droplets (64, 65). Of note, during feeding, secreted insulin induces the uptake of circulating glucose by adipocytes, which can enter either glycolysis or the *de novo* lipogenesis pathways, which produce important lipid substrates such as glycerol-3-phosphate (Gro3P) and FAs respectively (65). Also, insulin signalization regulates TG synthesis by upregulating lipogenic enzymes and simultaneously inhibiting lipid catabolism (63).

Secondly, during fasting or exercise, adipocyte TGs are broken down into three FFAs and glycerol to be used a fuel. The first lipase involved in this process is ATGL, which hydrolyzes TG into either *sn*2,3-DAG or *sn*1,3-DAG and FFA (62). Then, HSL hydrolyzes DAGs into MAG and FFAs, and finally

MAGL cleaves MAG into glycerol and FFAs (65). FFAs can be transported into mitochondria to produce acetyl-CoA through the β-oxidation, which is used to generate energy through the citric acid cycle in the adipocytes (63). FFAs can also be secreted into the circulation to be absorbed by the metabolically active tissues and will be oxidized to generate ATP (adenosine triphosphate), and released-glycerol can enter the gluconeogenesis in the liver (64, 65).

Finally, fat catabolism and anabolism pathways are interlinked into a metabolic cycle termed GL/FFA cycle, which connects the glucose and fat metabolism and regulates various physiological and biological processes (61). In the same trend, GL/FFA cycle has been found to be implicated in the pathogenesis of metabolic diseases like T2D, obesity and cancer (61).

1.3.3.2. Glycerolipid/Free fatty acid cycle

GL/FFA cycle is a metabolic machinery comprised of lipogenesis and lipolysis arms (**Figure 5**). As the operation of lipogenesis and lipolysis leads to the formation and hydrolysis of GL, coupled with net breakdown of ATP, this GL/FFA cycle produces heat, and is considered "futile". However, inasmuch as the GL/FFA cycle generates several lipid intermediates and signals that are essential for cellular structure as well as functions, the usage of ATP for the operation of this cycle can be viewed as the "currency" the cell pays for generating these signals as well as heat (61). The different steps of the GL/FFA cycle are detailed below.

Lipogenesis is an anabolic process through which TG is synthesized. The different enzymes involved in this process are the acyl-CoA synthase (ACSL), the glycerophosphate acyltransferase (GPAT), the 1-acyl-*sn*-Gro3P acyltransferase (AGPAT), the phosphatidic acid phosphatase (PAP) and the DAG acyltransferase (DGAT). First, FFA, entering into the cell, is converted to fatty acyl-coenzyme A (FACoA) by the ACSL. FFAs arise either from the uptake of exogenous FFA, intracellular lipolysis, or *de novo* lipogenesis from glucose (61). Then, the GPAT isoenzymes (GPAT 1 to 4) condense FACoA and Gro3P, arising from glycolysis or glyceroneogenesis, into lysophosphatidic acid (LPA). AGPAT isoenzymes esterify LPA using another molecule of FACoA to form phosphatidic acid (PA). Next, PA is converted in *sn*1,2-DAG by lipins, also known as PAPs (61). At this step, PA and *sn*1,2-DAG can also be used to produce phospholipids (PL). The last

reaction of the anabolic lipogenesis process of GL/FFA cycle is completed by DAG acyltransferases (DGAT1 and 2), using *sn*1,2-DAG and FACoA to produce TG (61).

The catabolic lipolytic segment of the GL/FFA cycle results in the sequential hydrolysis of TG ester bonds by different lipases : ATGL, HSL, MAGL and α/β-hydrolase domain 6 (ABHD6). First, ATGL hydrolyzes the first ester bond at the *sn*1 position of the TG molecule to give *sn*2,3-DAG and FFA. *sn*2,3-DAG is hydrolyzed by HSL to form either *sn*2-MAG and FFA. Subsequent hydrolysis of 2-MAG is conducted by MAGL or ABHD6 to generate FFA and glycerol and to complete the cycle (61). Glycerol, thus produced, is converted back to Gro3P by glycerokinase to be recycled back into the lipogenic segment of the cycle (61) .

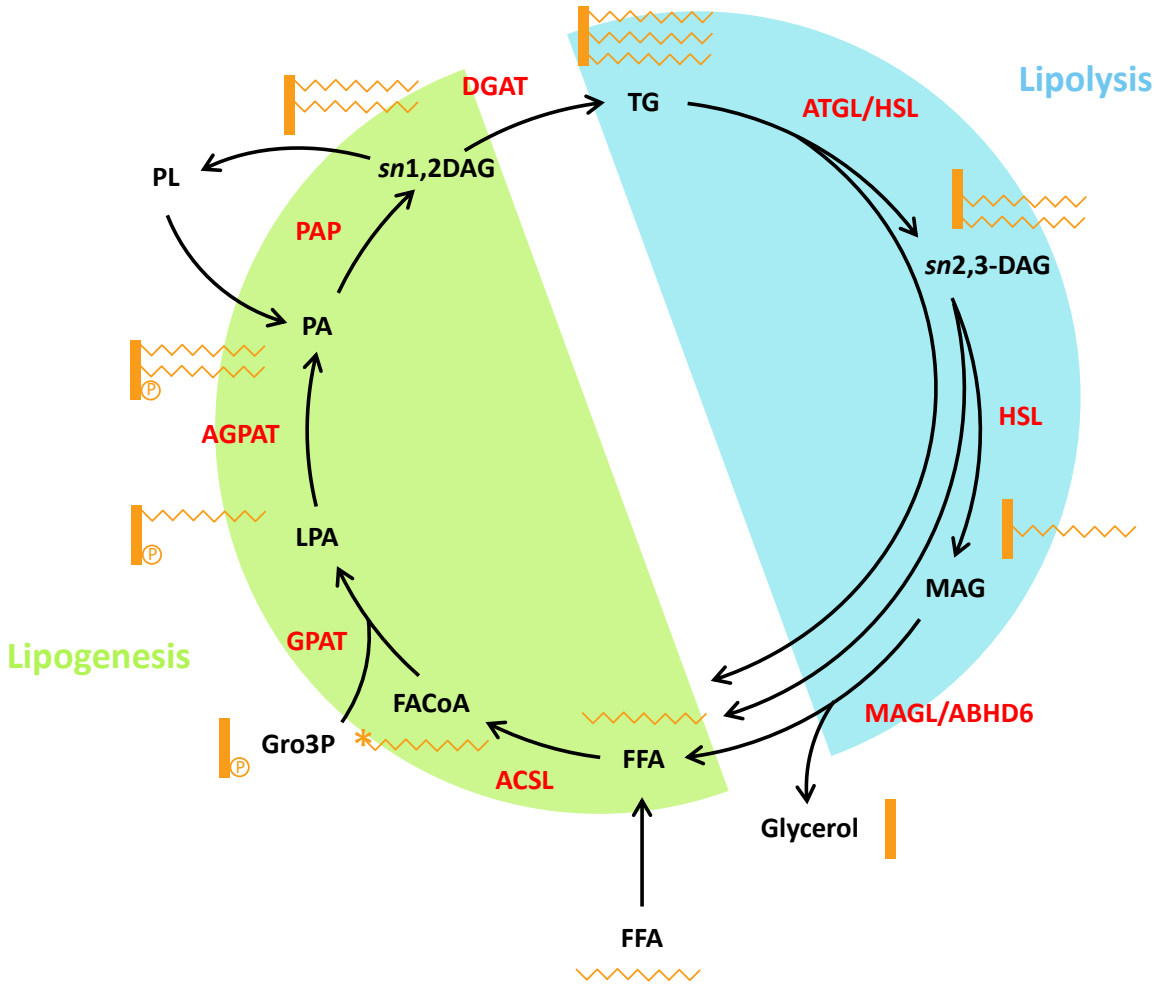

Figure 5. GL/FFA cycle enzymes and substrates.

The scheme depicts the GL/FFA cycling anabolic (lipogenesis) and catabolic (lipolysis) processes and corresponding enzymes. FACoA is formed by long-chain ACSL from FFA, and then partitioned into the generation of LPA through the condensation with glucose-derived Gly3P by GPAT. LPA is further converted by AGPAT to PA, which consequently gives rise to sn1,2-DAG by the action of PAP. Further DAG is converted to TG by enzymatic activity of DGAT. Through lipolysis, ATGL and/or HSL hydrolyzes TG to sn2,3-DAG which later breaks down to MAG by HSL. MAG is hydrolyzed by MAGL and ABHD6 to FFA and glycerol, which is secreted out of the cell. (figure modified from Prentki & Madiraju, 2008) (61).

1.4. Role of ABHD6 in obesity-mediated adipose tissue inflammation

Disturbances in lipid metabolism contribute to the development of metabolic complications, such as obesity, T2D, and NAFLD. Therefore, it is important to understand the precise mechanisms underlying the lipolytic and lipogenic pathways and their components (62).

1.4.1. ABHD6 gene and enzyme

ABHD6 is a type II integral membrane protein of 337 amino acid residues, classified as a serine hydrolase (66). The gene encoding ABHD6 in humans is divided in 10 exons and found on chromosome 3p14.3. The enzyme is folded in 8 β-strands, enclosed by α-helices and connected by loops. The catalytic site of the enzyme consists of the amino acid residues Ser148-Asp278-His306 triad and found on the loop region facing the cytoplasmic side, and the mutation of Ser148 into an alanine residue inhibits ABHD6 activity (62). ABHD6 plays various biological roles in different tissues. In addition to MAG, ABHD6 can hydrolyze few other lipid substrates such as lysophosphatidylcholine, LPA, and bis(monoacylglycero)phosphate. It is important to point out that ABHD6 is an ubiquitous enzyme, but its mRNA expression is higher in liver, kidney, and ovary in human, and in BAT, small intestine and brain in mice. Our previous studies showed that ABHD6 is also highly expressed in pancreatic islet β-cells compared to MAGL (66, 67). Although ABHD6 and MAGL catalyze the same reaction, ABHD6 inhibition or deletion does not cause compensatory

change in MAGL expression or function in the brain. Similarly, peripheral tissue deletion of ABHD6 using antisense oligonucleotides (ASOs), has no compensatory change in MAGL activity or expression in the liver (66, 68-70). Likewise, MAGL global deletion is not compensated by ABHD6, ABHD12 or HSL in brain, liver and AT (71). Few pharmacological inhibitors of ABHD6 have been identified, such as WWL70, a selective carbamate-based inhibitor, or KT203, an triazole urea-based inhibitor with high potency (72, 73). Other lipases, like ABHD12 and ABHD2, have been found to have specific hydrolysis roles of 2-arachidonoylglycerol (2-AG) in brain, particularly in the microglia, and spermatozoa respectively (62). Actually, ABHD12 is poorly characterized but mutations into ABHD12 gene have been shown to cause a neurodegenerative disease called PHARC (polyneuropathy, hearing loss, ataxia, retinitis pigmentosa and cataract) (74). ABHD2, despite its physiological function in fertilization of the spermatozoa, has been linked to pathological processes such as emphysema, atherosclerosis and virus propagation, and selective inhibitors for this enzyme are not yet available (74).

1.4.2. Monoacylglycerol metabolism and signaling

During fat digestion, TG are hydrolyzed into FFA and 2-MAG by pancreatic lipase in the intestinal lumen and are absorbed by intestinal epithelial cells which re-synthesize TG and assemble chylomicrons. The chylomicrons with TG are then released into the blood. The circulating chylomicron-associated TG are consequently hydrolyzed by plasma lipoprotein lipase into 2,3-DAG, 2-MAG, and finally FFA and glycerol. The FFA are taken up by the tissues and stored as TG in lipid droplets in the cells. Stored TG is hydrolyzed through the catabolic segment of GL/FFA cycle, depending on the metabolic needs of the cell.

1.4.2.1. Biosynthesis and degradation of MAG

Depending on the position of acyl chain on the glycerol backbone, there are two stereochemical isoforms of MAG: 1-MAG, with FA in the *sn1* or *sn3* positions and 2-MAG with FA in the *sn2* position of the glycerol backbone. MAG is mostly generated through lipolysis cascade and its stereoisomer structure depends on the enzymes involved and the order of reactions during TG hydrolysis. First, depending on the presence or absence of its co-activator CGI58, ATGL produces either *sn*2,3-DAG or *sn*1,3-DAG, respectively, and FFA (75). Under basal conditions, ATGL acts

alone, and generates *sn*1,3-DAG by hydrolyzing TG at *sn2* position. However, during stimulated-lipolysis, ATGL synergizes with its co-activator CGI58 to produce *sn*2,3-DAG, by hydrolyzing TG at the *sn1* position. Action of HSL on *sn*1,3-DAG generates 1-MAG, while its action on *sn*2,3-DAG generates 2-MAG (62). In addition to its formation from TG hydrolysis, 2-MAG can also arise from *sn*1,2-DAG, produced from membrane-associated PL, by phospholipase C, with its subsequent hydrolysis by membrane associated DAG lipases or cytosolic HSL into 2-MAG and FFA (76). Production of 1-MAG can also occur via the hydrolysis of LPA by LPA phosphatases (62). MAGL was found to hydrolyze both 1- and 2-MAG non-specifically, whereas ABHD6 has substrate preference for 1-MAG (67). Studies from our lab showed that suppression of ABHD6 induces 1-MAG accumulation in pancreatic islets, INS-1 cells, WAT and BAT and implicated 1-MAG in different cellular signaling pathways (67, 77).

1.4.2.2. Signaling roles of MAG

Endocannabinoid 2-AG was the first ABHD6 substrate to be identified in the CNS (66, 69). 2-AG is an agonist of cannabinoid (CB) receptors 1 and 2, which are implicated in the regulation of satiety and energy metabolism in brain (78, 79). CB2 receptor is also highly expressed in various immune cells, including macrophages and monocytes, and its activation by 2-AG could have anti-inflammatory effect or pro-inflammatory effect depending on the cell types and conditions (62, 80-82). On the other hand, 2-oleoylglycerol (another 2-MAG) was found to have a role in glucose and insulin homeostasis in the intestine through its binding to GPR119, a G protein-coupled receptor (GPR) implicated in the control of cyclic AMP levels in the cell and to regulate the secretion and release of GLP1 (Glucagon-like Peptide-1) from the intestinal L-cells (62). A recent study has suggested that RBP2 in the intestine can bind with 2-MAG and also 1-MAG in its retinoid binding site and this interaction has ramifications in the secretion of glucose-dependent insulinotropic polypeptide (GIP) because RBP2-KO mice exhibit elevated levels of 2-MAG in the proximal intestine and elevated GIP levels in the blood (83). Finally, we demonstrated that 1-MAG, which accumulates in ATs upon constitutive deletion of ABHD6 in whole-body in mice, can bind and activate PPARα and PPARγ (77). PPARs are actually activated by different lipid molecules. PPARα is present in several tissues and controls lipid and lipoprotein metabolism. PPARγ is a

master regulator of lipogenesis and adipocyte differentiation and also have a role in inflammation and cytokine secretion in the AT (84-86).

1.4.3. ABHD6 in obesity-induced inflammation

Several studies have identified physiological and pathological functions of ABHD6 in many tissues and organs (**Figure 6**). As discussed above, obesity is often associated with a systemic low-grade inflammation by increasing macrophage recruitment and polarization in the adipose depots (87). Furthermore, the hydrolysis of 2-AG by ABHD6 generates arachidonic acid, a precursor of prostaglandins, which are involved in inflammatory responses (88). Additionally, an *in vitro* study showed that ABHD6 inhibition is protective against LPS-stimulated inflammation in macrophages through the induction of prostaglandin-D2-glycerol (PDG2-G) ester synthesis. This pathway is mediated by cyclooxygenase-2 (COX-2) enzyme, and shown to be independent of CB receptors and PPARs activity (89). *In vivo*, ABHD6 inhibition with WWL70 significantly reduced the expression of the pro-inflammatory cytokines IL-1β, IL-6 and MCP1 in the cerebellum, liver and lungs of mice challenged with LPS. Further, it was not the accumulation of 2-AG upon ABHD6 inhibition that was in cause, but the conversion of 2-AG into PDG2-G by COX-2 that induced the anti-inflammatory effect of ABHD6 inhibition in those tissues for the most part (89). Finally, a study from Prentki lab revealed that the global deletion of ABHD6 in mice fed with HFD induces the elevation of anti-inflammatory cytokines and the reduction of pro-inflammatory cytokines in the plasma (77). However, the specific role of ABHD6 in immune cells and obesity-induced inflammation is still unknown.

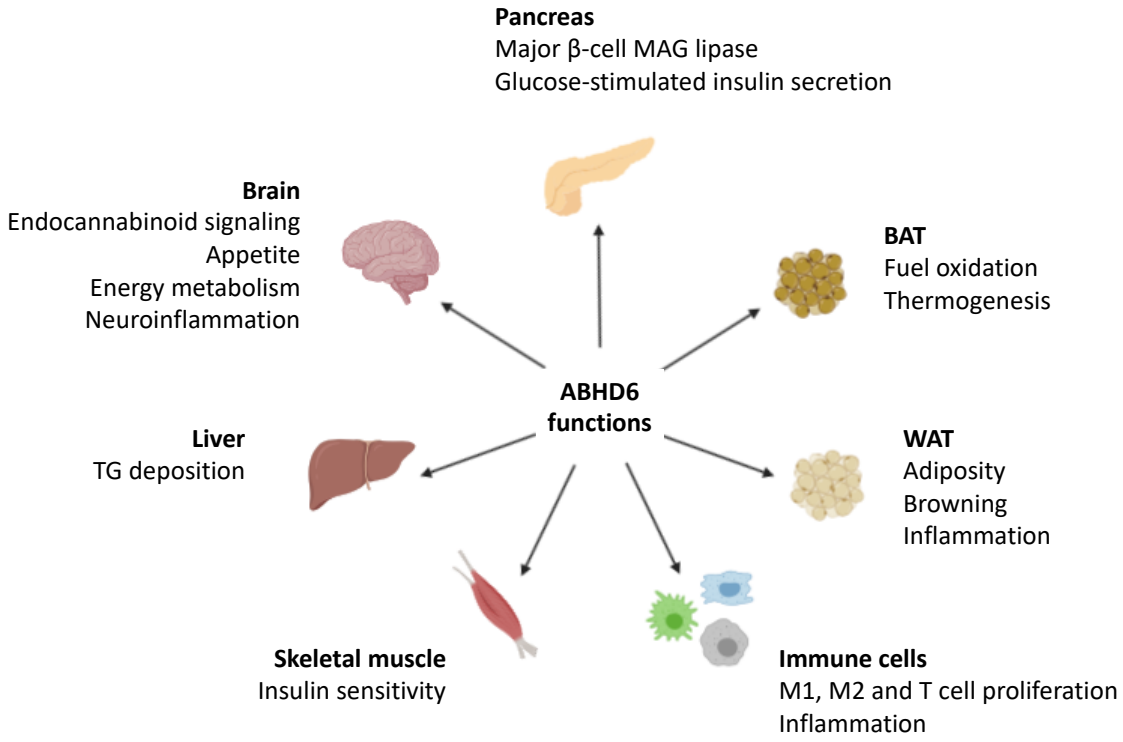

Figure 6. ABHD6 pathophysiological functions.

ABHD6 is involved in several organs and tissues and in many physiological and pathological functions (figure inspired by Poursharifi et al. review, 2017) (62).

1-MAG, accumulating upon ABHD6 inhibition, has been found to have an important role in adipocyte browning and beiging and energy expenditure. Previous study from our lab showed that ABHD6 inhibition in differentiated preadipocytes induces the expression of brown adipose markers such as UCP1 (77). In the same study, our lab demonstrated that ABHD6 deletion in mice protects them from HFD induced obesity and associated complications. Some of these beneficial effects include: reduced body weight gain and food intake, protection from hepatic steatosis, improved insulin and glucose tolerance, insulin-independent glucose uptake in AT and muscle, enhanced energy expenditure and increased WAT browning and BAT activation (77). In this study ABHD6 deletion was shown to result in an increase in lipolysis derived 1-MAG, which induces

adipose browning via PPARα and PPARγ activation. Thus, ABHD6 has been proposed to be a potential therapeutic target for obesity and T2D (77).

1.4.4. Role of ABHD6 in neuroinflammation

Apart from its role in AT and immune cells, ABHD6 role in neuroinflammatory and neurodegenerative diseases, as well as in the CNS-controlled energy balance are also studied (62). Locally increased endogenous 2-AG, by ABHD6 inhibition in an experimental autoimmune encephalomyelitis mouse model, led to a reduction in CD4+ T cell infiltration, microglia accumulation, pro-inflammatory cytokines, demyelination and axonal injury in the spinal cord (90). Another study showed that inhibition of ABHD6 with WWL70 in a traumatic brain injury mouse model reduced the expression of iNOS (Inducible nitric oxide synthase) and COX-2 and enhanced Arg-1 expression in the ipsilateral cortex, which suggests a switch from M1 to M2 phenotype in the microglia macrophages (91). To conclude, ABHD6 has been linked to many physiological and pathological processes, and its pharmacological inhibition could have therapeutic effects against obesity-induced inflammation and its complications, as well as neuroinflammatory diseases.

1.5. Rationale and hypothesis

Obesity is a major risk factor for metabolic diseases, including T2D, non-alcoholic steatohepatitis, cardiovascular diseases and inflammatory disorders (2, 3). These comorbidities are associated with the development of a low-grade chronic inflammation induced by maladaptive inflammatory response to a long-term positive energy balance (3). However, the prevalence of obesity continues to increase, causing a huge burden to our society and healthcare costs to rise. Therefore, it is crucial to better understand the cellular pathways and molecular mechanisms implicated in obesity and its associated inflammation in order to develop new therapeutic strategies.

ABHD6 is a ubiquitous monoacylglycerol lipase, catalyzing the last step of the lipolysis arm of the GL/FFA cycle. After its discovery in brain, ABHD6 was shown to contribute significantly to MAG hydrolysis in different cells/tissues, and also to play a role in the pathogenesis of metabolic diseases and some cancers (62). Studies from our lab showed that whole-body ABHD6 deletion in mice is protective against HFD-induced obesity via reduced body weight gain, protection from hepatic steatosis, improved insulin and glucose tolerance, and increased WAT browning and BAT activation (77). A recent study from our lab demonstrated that AT-specific ABHD6 deletion protects mice from cold exposure by enhancing WAT thermogenic programs (92). It was found that adipose ABHD6 deletion causes accumulation of adipocyte nuclear 2-MAG, which through the activation of PPARα and PPARγ, induces GL/FFA cycling in gonadal WAT, during cold challenge (92). Moreover, others showed the protective effect of pharmacological inhibition of ABHD6 against LPS-stimulated inflammation in macrophages *in vitro*, and also in the cerebellum, liver and lungs after a LPS challenge *in vivo* (89). However, the role of ABHD6 in diet-induced AT inflammation and macrophage polarization remains unexplored. We hypothesized that **suppression of ABHD6 is protective against HFD-induced AT inflammation by regulating the AT macrophage phenotype**. This hypothesis has been examined by addressing the following aims:

1) To assess the immunometabolic role of ABHD6 in obesity-induced AT chronic inflammation in mice;

2) To clarify the regulatory role of ABHD6 in the acute macrophage activation/polarization under LPS-induced inflammation.

To address these aims, we employed genetic and pharmacological approaches: whole-body ABHD6 KO mice generated for *in vivo* and *ex-vivo* studies, the ABHD6 inhibitor KT203 and macrophages cell lines used for *in vitro* studies. To induce chronic low-grade inflammation, whole body ABHD6-knockout animals and wild-type litter mates were put on 60% HFD for 17 weeks. Here, as it is well known that female mice are protected from HFD-induced inflammation, we only used male mice (93). In addition, acute inflammatory responses were studied using macrophage cell lines after treatment with LPS for 24 h.

The results from these studies are aimed at a better understanding of the role of AT ABHD6 in the dysregulation of metabolic and inflammatory pathways in obesity and to delineate the underlying cellular and molecular mechanisms of the protective effects of its suppression.

Chapter 2 - Methods

2.1. Animals

2.1.1. Whole-body ABHD6 KO mice generation

All procedures were approved by the Institutional Committee for the Protection of Animals in the CRCHUM. Whole-body (WB) ABHD6-KO mice were generated on pure C57/BL6N background by employing "KO-first" design as previously described before (67, 94). Briefly, the "KO first" allele is generated embryonic stem (ES) cells by splicing exons to a splice acceptor in the targeting cassette which will induce the inactivation of the gene function. The ES cells (JM8A3.N1 (Agouti), derived from C57/BL6N mice), with conditional vector targeting for ABHD6 (HEPD0651_8_C07) were obtained from European Conditional Mouse Mutagenesis Program, Germany. Further details on the ES cells and vectors are available at http://www.knockoutmouse.org/martsearch/project/72228. Schematic of the conditional knockout-first cassette for producing ABHD6-KO mice is shown in **Figure 7A**. As detailed in the scheme, the intervening sequences (Neo cassette), that cause suppression of ABHD6 expression are introduced between exons 2 and 3 of ABHD6 gene. Because of the interfering Neo-cassette, transcription of ABHD6 gene is terminated after exon-2 and the resulting short, truncated mRNAs are degraded, leading to the loss of ABHD6 expression in the whole body. These mice are referred to as "Knockout-first" as the same line of mice can also be used by breeding with Flpo deleter mice to generate ABHD6-fl/fl mice for conditional deletion of ABHD6 in a tissue specific manner. Knockout-first WB-ABHD6-KO mice were generated in Mouse Biology Program, University of California, Davis. Positioning of primers for genotyping PCR is indicated (**Figure 7A**), for an anticipated 517 bp DNA fragment (with primers, loxP-F & R1) for floxed mutant mice and a 200bp fragment (with primers, wtF & wtR) for wild-type mice. Chromosomal DNA extracted from a piece of the tail was used for genotyping the WT and KO mice (3 weeks old). For the WT mice, the following primer sequences were used: forward (wtF) 5'- GCAGAAAGGAAAGTAATACCTTAAGAG-3' and reverse (wtR) 5'- AACATCTTAAAACTTAATGCTGATAGCTC-3'. Although these sequences are also present in the targeting vector, they are spaced far apart and do not give rise to the

anticipated PCR product in the mutant mice (**Figure 7B**). For the WB-ABHD6-KO mice, the following primer sequences were used : forward (loxP-F) 5'-GAGATGGCGCAACGCAATTAATG-3' and reverse (ABHD6-R1) 5'- CAAGTGATGCTATGTAACCTTGCCCC-3'. The KO mice give a mutated PCR product of 517 bp whereas WT PCR product is indicated by a 200 bp band (**Figure 7B**).

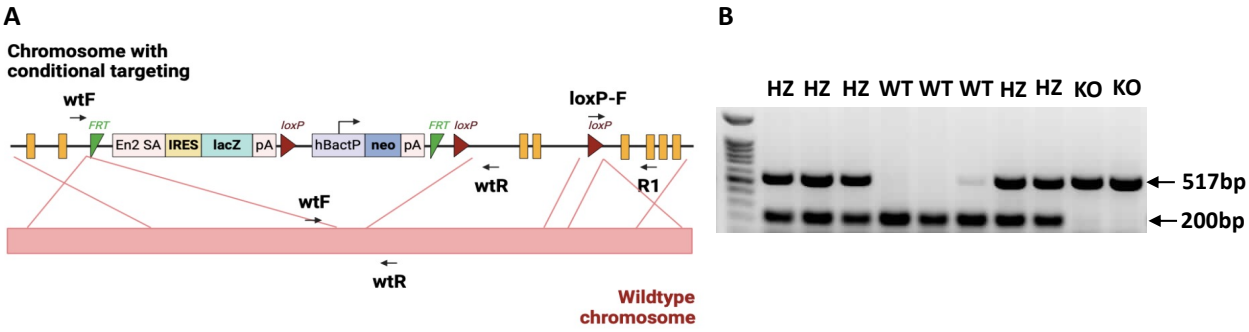

Figure 7. Generation and genotyping of WB-ABHD6-KO mice.

(A) Schematic of the conditional "KO-first" cassette for generating WB-ABHD6-KO mice. Positioning of the primers used for genotyping PCR are indicated : wtF and wtR primers for the WT mice giving a 200 bp fragment, and loxP-F and R1 primers for the mutant mice giving a 517 bp fragment (scheme modified from Zhao *et al*, 2014) (67). **(B)** Genotyping PCR amplification of chromosomal DNA from KO and WT mice tails (3 weeks of age). The 517 bp DNA fragment is corresponding to the -/- mice (WB-KO), the 200 bp fragment shows the +/+ mice (WT) and both fragments are from heterozygous +/- mice (HZ).

2.1.2. Type 2 diabetes *db/db* mice model

BKS.Cg-Dock7m$^{+/+}$Leprdb/J mice were purchased from the Jackson Laboratory (Mouse Strain Datasheet - 000642). Male mice (10 weeks of age), homozygous for *Leprdb* (*db/db* mice) and heterozygous for *Dock7m* (*db/+* mice) were used.

2.1.3. Mice maintenance

Mice were housed at room temperature (RT) (22°C) on a 12-hour light/12-hour dark cycle with free access to water and food (normal diet, ND) (Teklad Global 18% protein rodent diet irradiated 20-50KGy, Envigo) (**Appendix A.**).

2.2. *In vivo* studies on HFD-fed mice

2.2.1. HFD treatment

At weaning (4-5 weeks old), male wild-type (WT) and WB-ABHD6-KO mice were placed in individual cages and fed either chow diet or HFD (D12492i Rodent diet with 60% fat by energy, Research Diets) (**Appendix B.**) for 17 weeks (**Figure 8A**). Body weight and food intake were measured weekly. After 17 weeks, blood was collected from the tail vein for glucose measurement by a portable glucometer (Accu-check Advantage, Roche, Indianapolis, IN)., WB-ABHD6-KO and WT mice were sacrificed and tissues (iWAT, gWAT, BAT, liver, spleen, heart) and blood were collected. Plasma and tissue samples were kept at -80°C until processed.

2.2.2. Mouse adipose tissues

After 17 weeks on ND or HFD, interscapular BAT (BAT), visceral perigonadal WAT (gWAT) and subcutaneous inguinal WAT (iWAT) were collected from WT and WB-ABHD6-KO mice (**Figure 8B**). Male *db*/*db* and *db*/*+* mice were also sacrificed at 10 weeks of age on ND, and the gWAT was collected. ATs were either used freshly for gene and protein expression analysis, or digested with collagenase to isolate SVF as described in the next section.

2.2.3. Stromal Vascular Fraction isolation

Freshly isolated adipose tissues were processed for stromal vascular fraction (SVF) isolation (**Figure 8B**). Briefly, fat pads were collected in Krebs-Ringer bicarbonate HEPES buffer containing 10 mM HEPES, pH 7,4 (KRBH) and carefully minced into small pieces. Minced tissues were digested in the buffer containing 1 mg/mL collagenase type II (from *Clostridium histolyticum*) (C6885, Sigma-Aldrich) in KRBH buffer and 2% bovine serum albumin (BSA) (A6003, Sigma-Aldrich), (1 mg tissue/5 mL digestion buffer). The suspension was incubated at 37°C with constant shaking for 45 min. The supernatant (mature adipocytes) was discarded and the SVF fraction was pelleted by centrifugation (1500 rpm for 10 min), washed 3 times with KRBH buffer, and filtered (70 µm diameter). Obtained SVF cells were used freshly for flow cytometry.

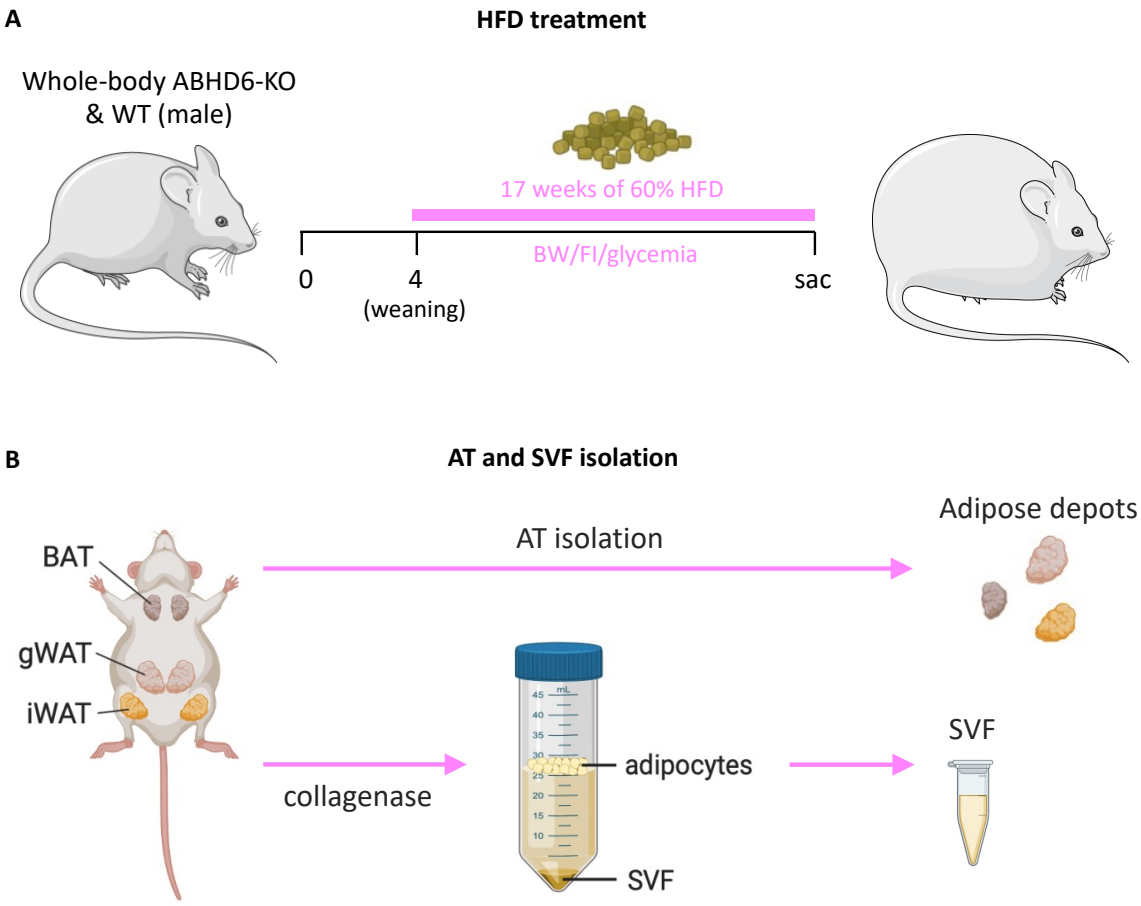

Figure 8. In vivo studies on HFD-fed mice.

(A) WB-ABHD6-KO and WT mice were fed HFD for 17 weeks, starting from weaning. Body weight (BW), food intake (FI) were measured weekly. They were sacrificed (sac) after 17 weeks on HFD and tissues were collected. **(B)** Simplified scheme showing the different adipose depots studied and AT/SVF isolation. BAT, gWAT and iWAT were collected. Fat depots were either used freshly for gene and protein expression, or digested with collagenase to isolated SVF for flow cytometry.

2.2.4. Tissue triglyceride content

Liver, spleen and heart triglyceride (TG) contents were determined for ectopic fat accumulation. This assay is based on the spectrophotometric measurement of glycerol released from the enzymatic hydrolysis of TG in the tissue homogenates. Briefly, tissues were homogenized in lysis buffer (20 mM Tris-HCl, pH 7,2, containing 150 mM NaCl, 1 mM EDTA, 1 mM EGTA, 1% v/v Triton

X-100, 0,1% SDS, and protease inhibitors), and 10 µL of crude tissue lysate was mixed with 100 µL of free glycerol reagent (F6428, Sigma-Aldrich) and 25 µL of triglyceride reagent (T2249, Sigma-Aldrich) in a 96-well plate. After 5 min incubation at 37°C, glycerol released from TG was measured by spectrophotometry at 450 nm and normalized with mg of protein.

2.3. *Ex-vivo* and *in vitro* studies

2.3.1. Flow cytometry

Adipose depots (iBAT, gWAT and iWAT) were isolated from WT and WB-ABHD6-KO mice after 17 weeks of 60% HFD. Fat depots were weighed and immediately processed for SVF isolation as described above. Macrophage populations were assessed by flow cytometry as described before (95). Briefly, red blood cells (RBC) were depleted by incubating freshly isolated SVF pellet in RBC lysis buffer for 9 min on ice, followed by a 5 min centrifugation at 300 g. 1 x 10^6 SVF cells were resuspended in 100 µL of FACS (Fluorescence-activated cell sorting) buffer for a final concentration of 1 x 10^7 SVF cells/mL. Cells were stained using LIVE/DEAD™ Fixable Aqua Dead Cell Stain Kit (Invitrogen; 1 ul/mL) for 30 min at room temperature, incubated on ice with 1/100 Fc-block for 10 min, and then incubated with 100 µL of antibody staining cocktail (1/200 anti-CD45.2, 1/200 anti-F4/80, 1/500 anti-CD11b, 1/200 anti-CD11c and 1/50 anti-CD301) for 30 min at 4°C, protected from light. The stained SVF cells were washed, fixed with 2% paraformaldehyde, and then used for flow cytometry analysis (BD Fortessa flow cytometer equipped with FACS Diva software). Anti-CD45.2 was used for leukocyte staining, anti-F4/80 and anti-CD11b for total macrophages, and anti-CD11c and anti-CD301 bind with M1 and M2 macrophages, respectively. Antibodies are listed in appendix (**Appendix C.**). The data analysis was performed using FlowJo v10.

2.3.2. Peritoneal macrophages isolation and activation/polarization

Peritoneal macrophages (PMs) were isolated from the peritoneal cavity of WT and WB-ABHD6-KO male mice as described before (96). PMs were harvested by washing the cavity with 10 mL sterile cold 1X PBS and 2,0 x 10^5 cells/well were plated in 24-well plates in Dulbecco's minimal

essential media (DMEM) (Gibco) supplemented with 10% fetal bovine serum (FBS) (Gibco) and antibiotics (Penicillin/Streptomycin). After 1h, PMs were washed with warm 1X PBS and treated with either 100 ng/mL LPS (L4516, Sigma-Aldrich) or 10 ng/mL IL-4 (AF-214-14, Preprotech) for 24h. After the 24h treatment, media were collected and stored at -20°C for cytokine secretion measurement and macrophages were kept at -20°C until RNA extraction.

2.3.3. Macrophage cell lines activation/polarization

RAW264.7 and J774A.1 macrophage cells were cultured in DMEM and Roswell park memorial institute (RPMI) 1640 media respectively, both supplemented with 10% FBS and antibiotics (Penicillin/Streptomycin). 0,2 x 10^5 cells/well were plated in 24-well plates. After the cells reached 60% confluency, they were treated with 10 µM KT203 (ABHD6 inhibitor) (provided by Servier-France) for 1h before adding either 100 ng/mL LPS or 10 ng/mL IL-4 for 24h. After the 24h treatment, media was collected and stored at -20°C for cytokine secretion measurement. And cells were kept at -20°C until RNA extraction.

2.4. Tissues and cell analysis

2.4.1. Protein expression by immunoblotting

For immunoblotting, ATs were digested with a lysis buffer (20 mM Tris-HCl, pH 7,2, containing 150 mM NaCl, 1 mM EDTA, 1 mM EGTA, 1% v/v Triton X-100, 0,1% SDS, and protease inhibitors), and after protein quantification, 25-40 µg protein were used for Western blot analysis. ABHD6 expression was measured and normalized with β-actin. Antibodies are listed in appendix (**Appendix C.**).

2.4.2. RNA extraction and quantification

Adipose depots. For gene expression, ATs were homogenized in 1 mL cold Qiazol (Qiagen), then 200 µL chloroform was added. After centrifugation at 13 000 rpm for 15 min at 4°C, the upper phase (RNA) was collected and mixed with 1:1 70% ethanol. Total RNA was then isolated using the RNeasy Mini Kit (Qiagen). Following reverse transcription of 1 µg RNA to cDNA, gene

expression was assessed by quantitative PCR using SYBR Green (204145, QuantiTect), in duplicate and normalized to *18s*. *Abhd6*, *Tnfa*, *Mcp1*, *Cd11c*, *Arg1*, Mrc1 (Macrophage Mannose Receptor C-Type 1), *Col1a1* (Collagen type I alpha 1 chain), *Col5a1* (Collagen type V alpha 1 chain) and *Hif1a* were measured. Primer sequences are listed in appendix (**Appendix D.**).

Cells. For RNA extraction, RAW264.7 and J774A.1 macrophages or PMs were scraped in 300 µL cell lysis buffer and transferred to the QIAshredder mini-column to homogenize and filter insoluble cell debris from the cell lysate (Qiagen). Total RNA was then isolated using the RNeasy Mini Kit (Qiagen). Following reverse transcription of 1 µg RNA to cDNA, gene expression was assessed by quantitative PCR using SYBR Green, in duplicate and normalized to *Gapdh*. *Tnfa*, *Mcp1*, and *Arg1* were measured. Primer sequences are listed in appendix (**Appendix D.**).

2.4.3. Cytokine secretion analysis by ELISA

Cytokine secretion from RAW264.7 macrophages was assayed by ELISA using commercial kits (# AL505 AlphaLISA TNF, Perkin Elmer for TNFα, and ab208979 ELISA, Abcam for MCP-1).

2.5. Statistical analysis

Results are expressed as means ± SEM. All data were analyzed and plotted using GraphPad Prism 8 (GraphPad Software). Statistical differences between2 groups were assessed by unpaired two-tailed Student's *t* test, and between multiple groups were assessed by 1-way or 2-way ANOVA. A *P* value of less than 0,05 was considered statistically significant.

Chapter 3 - Results

3.1. The global role of ABHD6 in diet-induced chronic low-grade inflammation

3.1.1. ABHD6 expression in the ATs of obese and diabetic mice

In order to investigate the role of AT ABHD6 under diet-induced inflammation, we measured ABHD6 expression in different adipose depots of obese and diabetic male mice (**Figure 9A**). WB-ABHD6-KO mice fed HFD for 17 weeks exhibited an increased mRNA expression of ABHD6 in all fat depots (gonadal WAT (*P*=0,0481), inguinal WAT (*P*=0,0538) and BAT (*P*<0,0001)), compared to ND-fed mice (**Figure 9A**). Similarly, ABHD6 mRNA (*P*=0,0336) and protein levels (*P*=0,0187) were significantly higher in *db*/*db* mice compared to control mice (**Figure 9B**). These results demonstrated the upregulation of ABHD6 in mice adipose depots under inflammatory conditions as obesity or T2D.

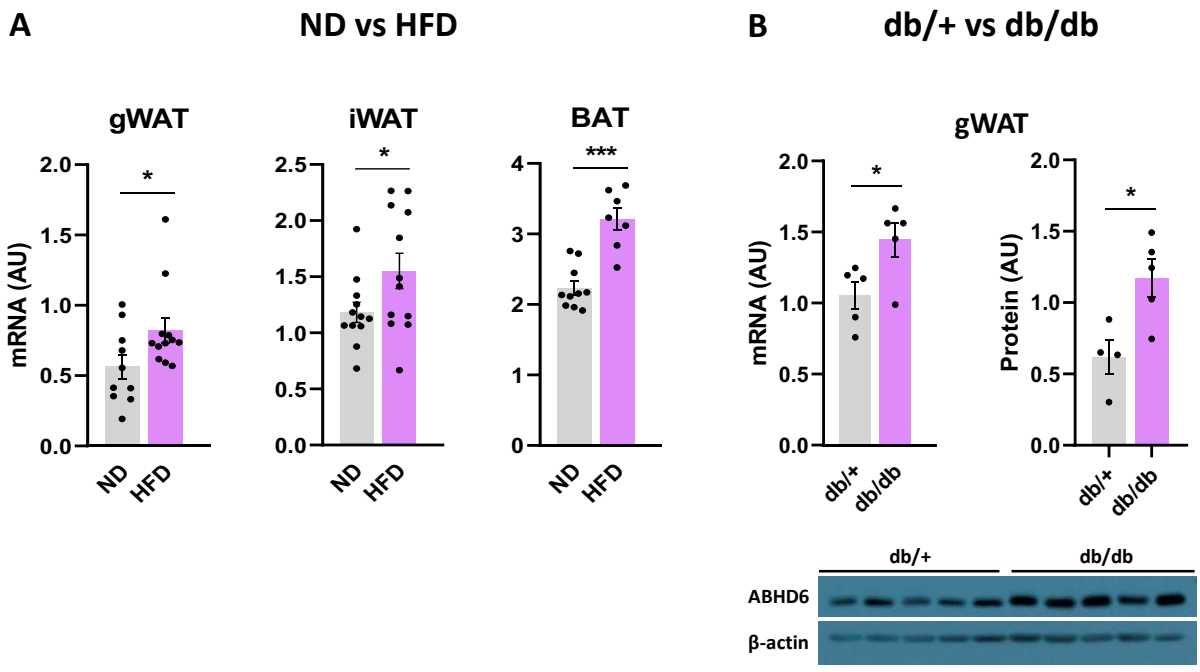

Figure 9. ABHD6 expression is upregulated in AT under inflammatory conditions.

(A) *Abhd6* mRNA expression in the ATs of WT mice fed ND or HFD for 17 weeks (*n* = 7-12 mice/group). **(B)** ABHD6 mRNA and protein levels in the gWAT of *db*/*+* and *db*/*db* mice at age 10 weeks (*n* = 4-5 mice/group). Gene expression analyses were run in duplicate and normalized to *18s*. Unpaired two-tailed Student's *t* test; effects of diet/genotype: **P* < 0,05; ****P* < 0,001.

3.1.2. ABHD6-KO mice are protected against HFD-obesity

Using global ABHD6-KO mice, we previously showed the beneficial effects of ABHD6 suppression in diet-induced obesity. Female and male mice fed HFD for 8 weeks showed reduced weight gain, improved glucose tolerance and insulin sensitivity, and reduced fat mass and liver steatosis (77). To assess the global role of ABHD6 in diet-induced inflammation, we used WB-ABHD6-KO and WT male mice fed with 60% HFD for 17 weeks from weaning (**Figure 10**). As reported before, WB-ABHD6-KO mice have a mild protection against diet-induced obesity shown by a significant reduction of their body weight and fed glycemia (*P*=0,0180), compared to WT HFD-fed mice (significant from week 9 to 17 under HFD) (**WB-ABHD6-KO mice are protected against HFD-induced obesity.**) (77). There was no difference in body weight between KO and WT mice under ND (**WB-ABHD6-KO mice are protected against HFD-induced obesity.**). No significant differences in dietary intake were observed among groups (**WB-ABHD6-KO mice are protected against HFD-induced obesity.**). Regarding the weight of tissues under HFD, iWAT (*P*=0,0196), liver (*P*=0,0380), spleen (*P*=0,0243) and heart (*P*=0,0393) weight were significantly reduced in the KO mice compared to the WT littermates (**WB-ABHD6-KO mice are protected against HFD-induced obesity.**). Accordingly, we observed reduced TG accumulation in both liver (*P*=0,0579) and spleen (*P*=0,0248) of HFD-fed KO mice, but not in heart, compared to controls (**WB-ABHD6-KO mice are protected against HFD-induced obesity.**). Further, due to more fat accumulation, the liver of the WT mice fed with HFD appears bigger and lighter, compared to the KO liver (**WB-ABHD6-KO mice are protected against HFD-induced obesity.**). These data confirmed the beneficial effects of ABHD6 deletion against diet-induced obesity in male mice.

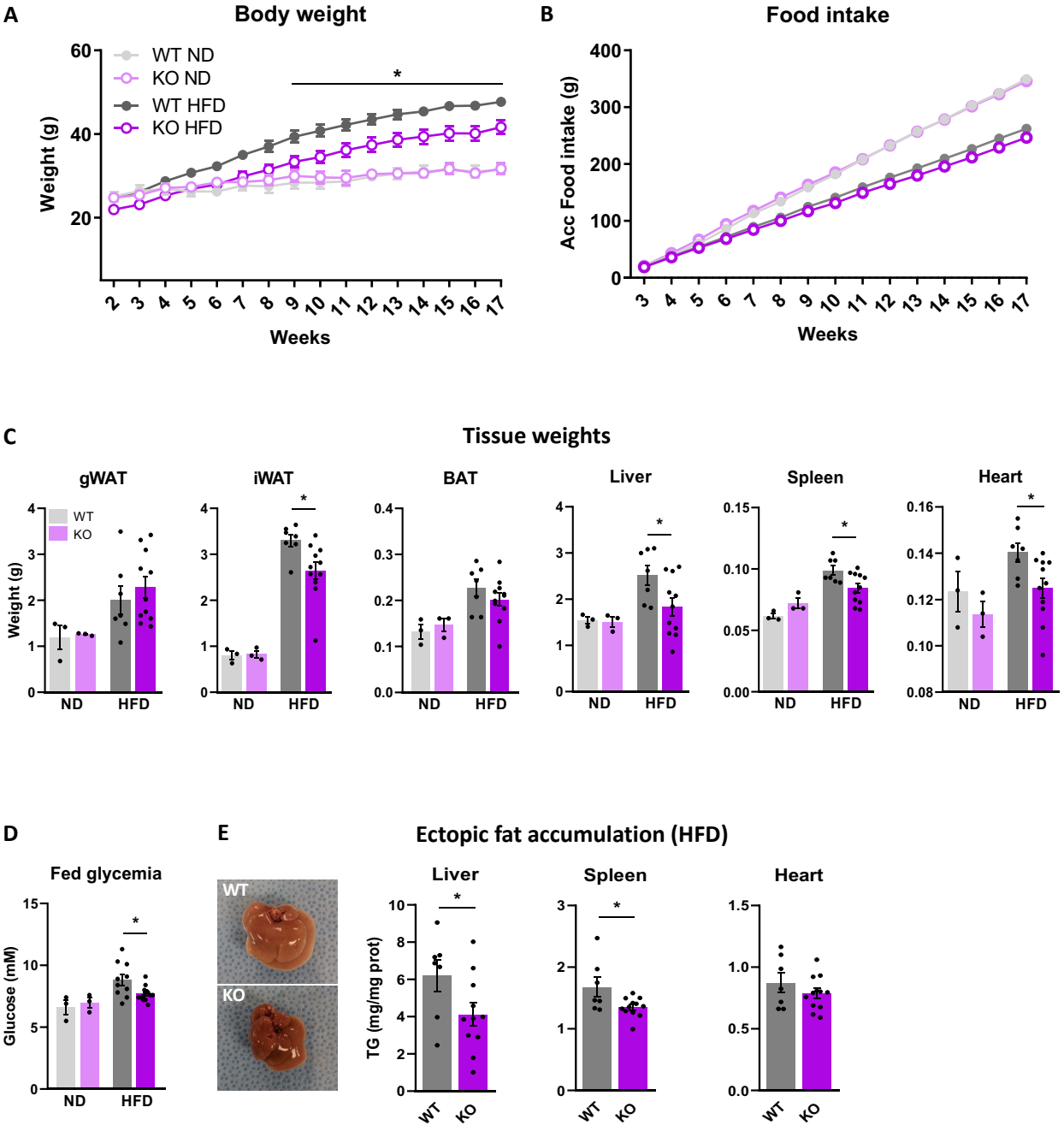

Figure 10. WB-ABHD6-KO mice are protected against HFD-induced obesity.

WT and WB-ABHD6-KO male mice were fed either with ND or HFD for 17 weeks (*n* = 3 for ND-fed mice; *n* = 7-11 for HFD-fed mice) **(A)** Body weight (BW). **(B)** Cumulative food intake (FI). **(C)** Tissue weights. **(D)** Fed glycemia measured in the blood from tail vein. **(E)** Liver, spleen and heart TG content in HFD-fed mice WT and KO (*n* = 7-11). 2-way ANOVA for BW and FI and 1-way

ANOVA for tissue weight, with Bonferroni's multiple comparison test ; unpaired two-tailed Student's *t* test for TG content; effects of genotype : *$P < 0,05$.

3.1.3. Global ABHD6 deletion effects on adipose tissue markers of inflammation, fibrosis and hypoxia

The long-term positive energy balance, taking place during the development of obesity, leads to AT hypoxia, inflammation and fibrosis (50-52). Eventually, these chronic events will induce adipocyte death, pro-inflammatory cytokines secretion and macrophage infiltration (23, 51). We previously revealed that HFD-fed mice with ABHD6 global deletion exhibit reduced pro-inflammatory cytokines levels and elevated anti-inflammatory cytokines levels in the plasma (77). However, ABHD6 role in diet-induced AT inflammation, fibrosis and hypoxia is still unknown.

To ascertain the effect of ABHD6 deletion in AT microenvironment health, we first examined the inflammatory profile of the three fat depots (iWAT, gWAT and BAT) isolated from WT and WB-ABHD6-KO mice fed with HFD for 17 weeks (**Figure 11**). *Tnfa* was decreased only in the BAT (P=0,0469) of KO mice compared to control (**Figure 11A**). However, diet-induced inflammation caused the downregulation of *Mcp1* in all the fat depots of ABHD6 KO mice compared to WT (P=0,0450 in gWAT; P=0,0011 in iWAT; P=0,0226 in BAT) (**Figure 11A**). *Cd11c*, a cell surface marker of M1-macrophages, was also reduced in the gWAT (P=0,0139), iWAT (P=0,0004) and BAT (P=0,0115) isolated from HFD KO mice, compared to control. Since ABHD6 deletion demonstrated a great impact on reducing pro-inflammatory responses in all the adipose depots, we next assessed if anti-inflammatory markers were equally upregulated. However, only *Arg1* was upregulated in the gWAT of KO mice (P=0,0139) and *Mrc1* was not changed between groups in the different fat depots (**Figure 11A**). Actually, Arg1 is mostly induced in M2-like macrophages and other lymphocytes in the AT microenvironment (21). We speculate that ABHD6 deletion reduces AT inflammation in the context of obesity.

We wondered if the AT inflammation reducing effect of ABHD6 deletion also impacted the obesity-induced AT fibrosis and hypoxia. Here we assessed two fibrosis markers, *Col1α1* and

Col5a1, and a major hypoxia marker, *Hif1a*, in the gWAT, iWAT and BAT fat depots. Type I collagen is the main collagen component of the AT and assembles to type V collagen to compose the framework of AT extracellular matrix. Both of those collagen are known to be upregulated in response to HFD (97). In a previous study from our lab, histology revealed that WB-ABHD6-KO mice exhibit smaller adipocytes in all fat depots in HFD-induced obesity, compared to WT mice (77). Thus, we chose *Col5a1* whose mRNA expression was reduced in all the ATs of ABHD6-KO mice (*P*=0,0532 in gWAT; *P*=0,0551 in iWAT; *P*=0,0518 in BAT), and *Col1a1,* which was decreased in BAT (*P*=0,0414), compared to WT mice fed HFD (**Figure 11B**). Finally, *Hif1a* was significantly downregulated in gWAT (*P*=0,0039) and BAT (*P*=0,0056), but not in iWAT from WB-ABHD6-KO mice compared to control mice (**Figure 11B**). Overall, the inflammation-reducing effect of ABHD6 deletion in the AT microenvironment is more pronounced in gWAT and BAT than iWAT, and is associated with an improvement of AT microenvironment health.

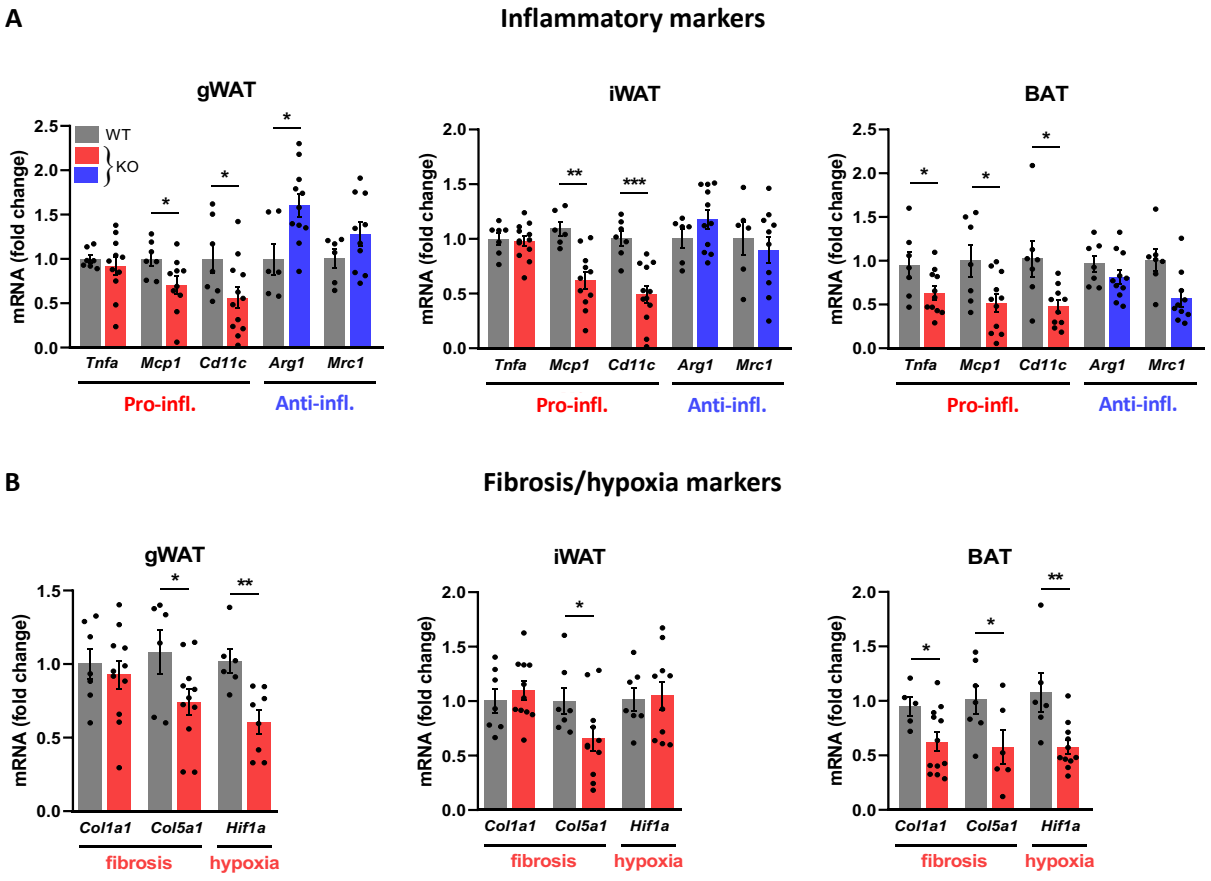

Figure 11. Global ABHD6 deletion alleviates AT inflammation, fibrosis and hypoxia.

(A) mRNA expression of pro-inflammatory (red, Pro-infl.) and anti-inflammatory (blue, Anti-infl.) markers in the ATs from WT and WB-ABHD6-KO mice fed HFD for 17 weeks (*n* = 7-11). **(B)** mRNA expression of fibrosis and hypoxia markers. Unpaired two-tailed Student's *t* test; effects of genotype : **P* < 0,05; ***P* < 0,01; ****P* < 0,001.

3.1.4. ABHD6 deletion reduces M1-macrophage population in gWAT and BAT

Our previous results demonstrated the effect of ABHD6 suppression in reducing diet-induced adipose inflammation. Thus, we wanted to assess if this reduction of pro-inflammatory cytokines levels was the result of changes in the leukocyte population cell composition. Thus, using flow cytometry, we analyzed the lymphocytes repartition in the SVF of gWAT, iWAT and BAT isolated from WB-ABHD6-KO and WT mice fed with HFD for 17 weeks (**Figure 12**).

In the SVF of the gWAT from HFD-fed ABHD6-KO mice, the leukocyte proportion ($CD45^+$ cells/ g of AT) and the total count of macrophages ($CD45^+$ $F4/80^{high}$ $CD11b^+$ cells) were not changed compared to the control (**Figure 12B**). However, the percentage of $CD45^+$ $F4/80^{high}$ $CD11b^+$ $CD11c^+$ $CD301^-$ cells (% M1 macrophages from $F4/80^{high}$ cells) was significantly reduced compared to controls (*P*=0,0412), but not the percentage of the $CD45^+$ $F4/80^{high}$ $CD11b^+$ $CD11c^-$ $CD301^+$ cells (% M2 macrophages from $F4/80^{high}$ cells) (**Figure 12B**). Overall, the ratio of M1/M2 macrophage count was significantly decreased compared to control (*P*=0,0385) (**Figure 12B**).

In the SVF of the iWAT from WB-KO mice fed-HFD, there was no change in the leukocyte proportion, total count of macrophages, M1 and M2 proportion in the AT macrophages and M1/M2 ratio (**Figure 12C,D**).

In the BAT SVF isolated from WB-ABHD6-KO HFD-fed mice, the number of leukocytes was significantly decreased (*P*=0,0083), with a decrease (non-significant) in the total number of macrophages, compared to WT (**Figure 12F**). Also, the percentage of M1 macrophages was decreased (*P*=0,0242), and conversely, the percentage of M2 macrophages was increased

(*P*=0,0400) compared to WT (**Figure 12F**). Finally, M1/M2 ratio was significantly diminished in the KO compared to control mice (*P*=0,0438) (**Figure 12F**).

The flow cytometry analysis goes along with previous data from this thesis showing a greater inflammatory-reducing effect of ABHD6 deletion in the AT microenvironment in gWAT and BAT than in iWAT (**Global ABHD6 deletion alleviates AT inflammation, fibrosis and hypoxia.**). Here, we can appreciate that ABHD6 deletion lessened the M1-like macrophage population in both gWAT and BAT, but not in iWAT.

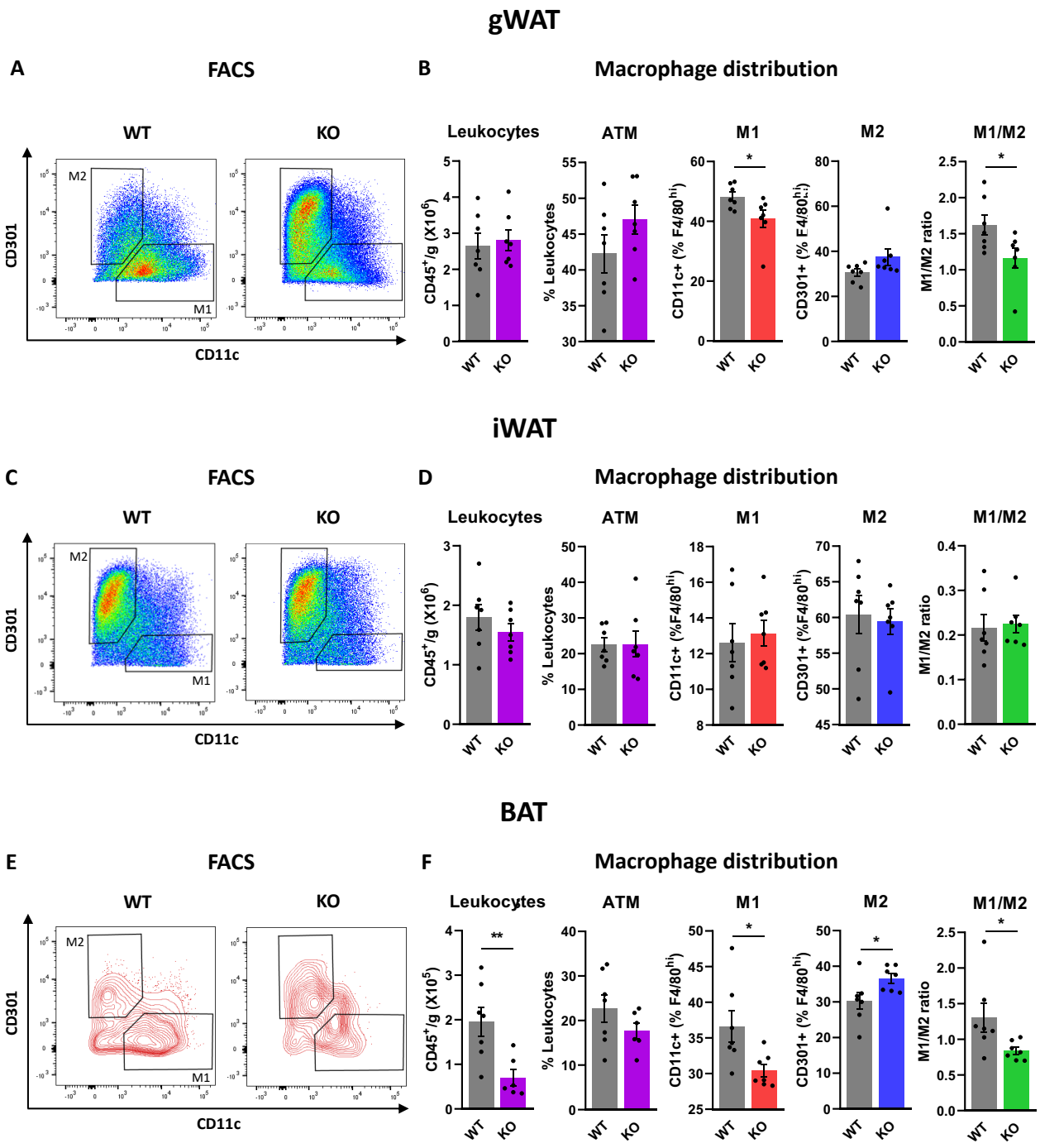

Figure 12. Global ABHD6 deletion reduces M1-macrophage polarization in gWAT and BAT.

Cell composition of gWAT, iWAT and BAT SVF from HFD-fed WT and KO mice (*n* = 7) were analyzed by flow cytometry. $CD45^+$ marker was used for leukocytes count; F4/80 and CD11b for macrophages; CD11c for M1 macrophages; CD301 for M2 macrophages. **(A,C,E)** Representative flow cytometry results of $CD45^+$ $F4/80^+$ $CD11b^+$ cells analyzed with anti-CD11c and anti-CD301

antibodies in the SVFs of gWAT, iWAT and BAT respectively. **(B,D,F)** Macrophage population in the SVFs of ATs from WT and KO mice. Leukocytes are represented by the number of $CD45^+$ cells per gram of AT. AT macrophages (ATM) are the percentage of $CD45^+$ $F4/80^{high}$ $CD11b^+$ cells in number compared to $CD45^+$ cells. M1 macrophages are the $CD45^+$ $F4/80^{high}$ $CD11b^+$ $CD11c^+$ $CD301^-$ cells, and M2 are the $CD45^+$ $F4/80^{high}$ $CD11b^+$ $CD11c^-$ $CD301^+$ cells. The analysis was done using FlowJo v10. Unpaired two-tailed Student's *t* test; effects of genotype : $*P < 0,05$; $**P < 0,01$.

3.2. The role of ABHD6 in macrophage polarization

Obesity is associated with a systemic low-grade inflammation by increasing macrophage recruitment and polarization in the ATs (87). Also, it has been shown that macrophage polarization toward M1 phenotype has a pathological role in inflammatory diseases (22). We discussed above that ABHD6 deletion induces a reduction in M1-like macrophages population in the gWAT and BAT from mice fed with HFD. Additionally, another study revealed that pharmacological inhibition of ABHD6 with WWL70 was protective against LPS-stimulated inflammation *in vitro* and *in vivo* (89). Here, we used primary macrophages from WB-ABHD6-KO mice and a more specific ABHD6 inhibitor (KT203) to assess the role of ABHD6 in macrophage activation and polarization under inflammatory conditions.

To assess the role of ABHD6 in macrophage polarization, we first inhibited ABHD6 with a pharmacological inhibitor, KT203, in two mice macrophage cell lines *in vitro*, RAW264.7 and J774A.1, and induced their polarization toward M1-like phenotype with LPS or toward M2-like phenotype with IL-4. Then, we measured M1 and M2 markers usually involved in the polarization, such as TNFα and MCP1 for M1-macrophages and Arg-1 for M2-macrophages (**Figure 13**). In both macrophage cell lines stimulated with 100 ng/mL LPS for 24h, pharmacological inhibition of ABHD6 with 10 mM KT203 induced a downregulation of *Tnfa* and *Mcp1* mRNA expression (P=0,009 and 0,0085 respectively for RAW264.7; P=0,0004 and <0,0001 respectively for J774A.1) and promoted Arg1 expression (P<0,0001 for both RAW264.7 and J774A.1) (**Figure 13A,C**). We further confirmed these results by measuring TNFα and MCP1 secretion from LPS-stimulated

RAW264.7 macrophages in their culture medium. Accordingly, both TNFα (*P*=0,0430) and MCP1 (*P*<0,0001) protein expressions were reduced in the media of macrophages treated with 10 mM KT203 (**Figure 13F**). However, pharmacological inhibition of ABHD6 with KT203 did not promote M2-polarization in both cell lines induced with 10 ng/mL IL-4, but mildly lowered IL-4-induced *Arg1* upregulation (**Figure 13B,D**). Next, in order to confirm the pro-inflammatory role of ABHD6 observed *in vitro*, we isolated and cultured primary peritoneal macrophages from WB-ABHD6-KO and WT mice (8 weeks of age), treated them with 100 ng/mL LPS for 24h, and measured pro- and anti-inflammatory markers. Under LPS-induced acute inflammation, ABHD6 deletion significantly decreased LPS-induced *Mcp1* upregulation (*P*<0,0001) and promoted *Arg1* mRNA expression (*P*=0,0486), similarly to macrophages cell lines (**Figure 13E**). Overall, these data revealed that ABHD6 possesses a proinflammatory role in macrophages and its inhibition induces a switch from M1-polarization to an anti-inflammatory M2-polarization in macrophages under LPS-induced acute inflammation.

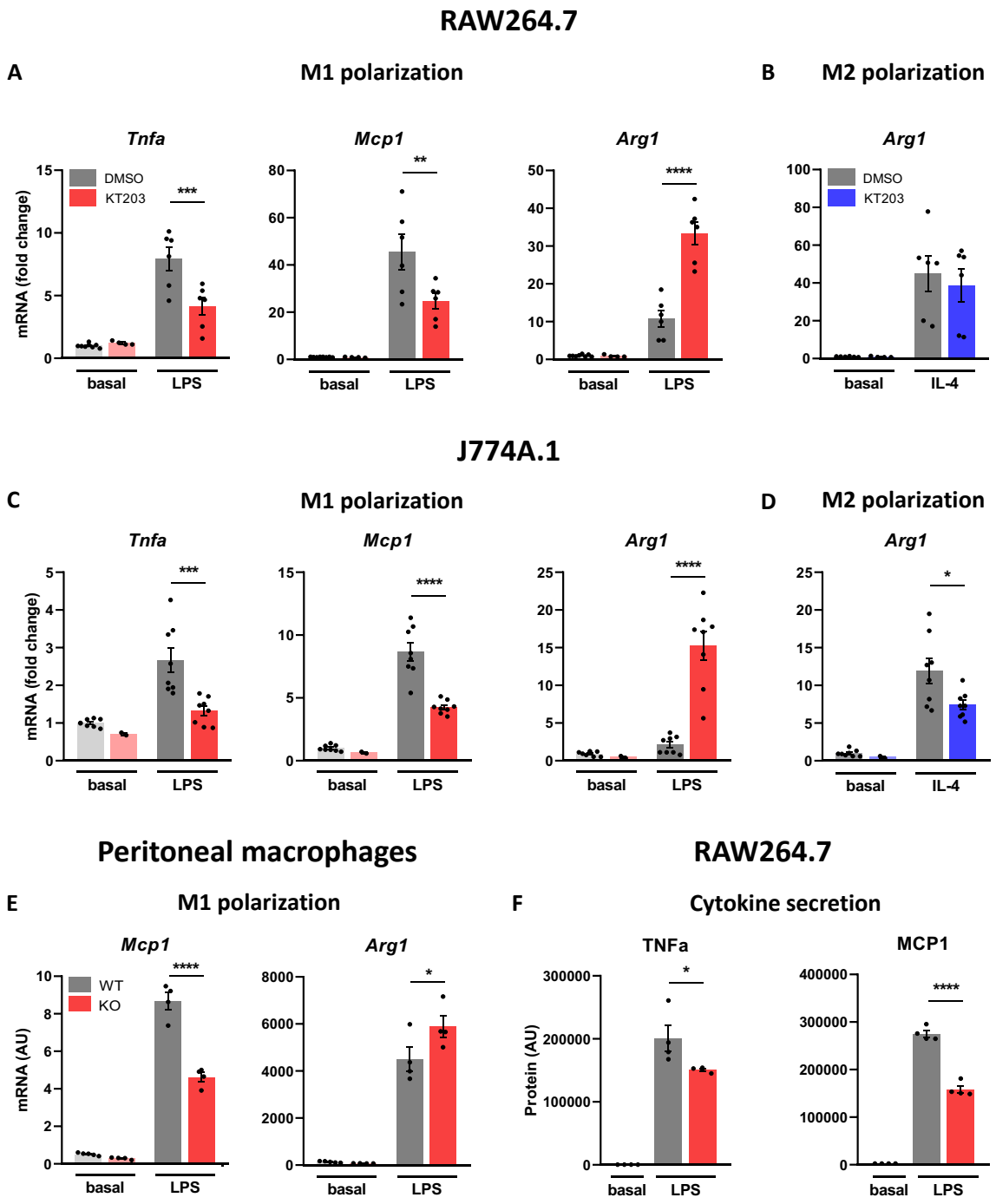

Figure 13. Pharmacological inhibition/deletion of ABHD6 in macrophages prevents LPS-induced M1 polarization and promotes M2 polarization.

RAW264.7 and J774A.1 cells were polarized for 24h with 100 ng/mL LPS (M1) or 10 ng/mL IL-4 (M2), with or without ABHD6 inhibitor KT203 (10 mM). Peritoneal macrophages were isolated from WT and WB-ABHD6-KO mice at 8 weeks of age, cultured and polarized with LPS 100 ng/mL

for 24h (*n* = 6-8 wells/group). **(A,C)** mRNA expression of pro-inflammatory M1 (*Tnfa* and *Mcp1*) and anti-inflammatory M2 marker (*Arg1*) from LPS-stimulated RAW264.7 and J774A.1 cells respectively, **(B,D)** *Arg1* mRNA expression from IL-4-stimulated RAW264.7 and J774A.1 cells respectively, in the presence or absence of KT203. **(E)** mRNA expression of *Mcp1* and *Arg1* of peritoneal macrophages isolated from WT and ABHD6-KO mice, treated with LPS for 24h. **(F)** TNFa and MCP1 release from LPS-stimulated RAW264.7 macrophages, in the presence or absence of KT203. mRNA expressions are normalized to *Gapdh* mRNA level. 1-way ANOVA and Tukey's post hoc test; effects of polarization/genotype : **P* < 0,05; ***P* < 0,01; ****P* < 0,001; *****P* < 0,0001.

Chapter 4 - Discussion

Maladaptive inflammatory responses to the long-term positive energy balance result in the development of a low-grade chronic inflammation, also known as meta-inflammation (3). AT-resident macrophages have been found to contribute greatly to the diet-induced low-grade inflammation (4-7, 11, 12). Macrophages are highly plastic cells influenced by adipokines, cytokines, hormones and fuel availability of the AT microenvironment. Thus, AT macrophage number and their activation state determine the metabolic health (6, 25). Therefore, understanding the mechanisms involved in the pathophysiology of AT-resident macrophages in obesity may provide new therapeutic strategies for obesity complications.

Studies from the Prentki laboratory and others have previously shown the beneficial effect of suppression of the ABHD6 against obesity, T2D, and other inflammatory disorders (62, 77). Moreover, pharmacological inhibition of ABHD6 has also been shown to be protective against LPS-stimulated inflammation in macrophages *in vitro* and in the cerebellum, liver and lungs *in vivo* (89). However, the role of ABHD6 in diet-induced AT inflammation and AT-resident macrophage polarization is not precisely known.

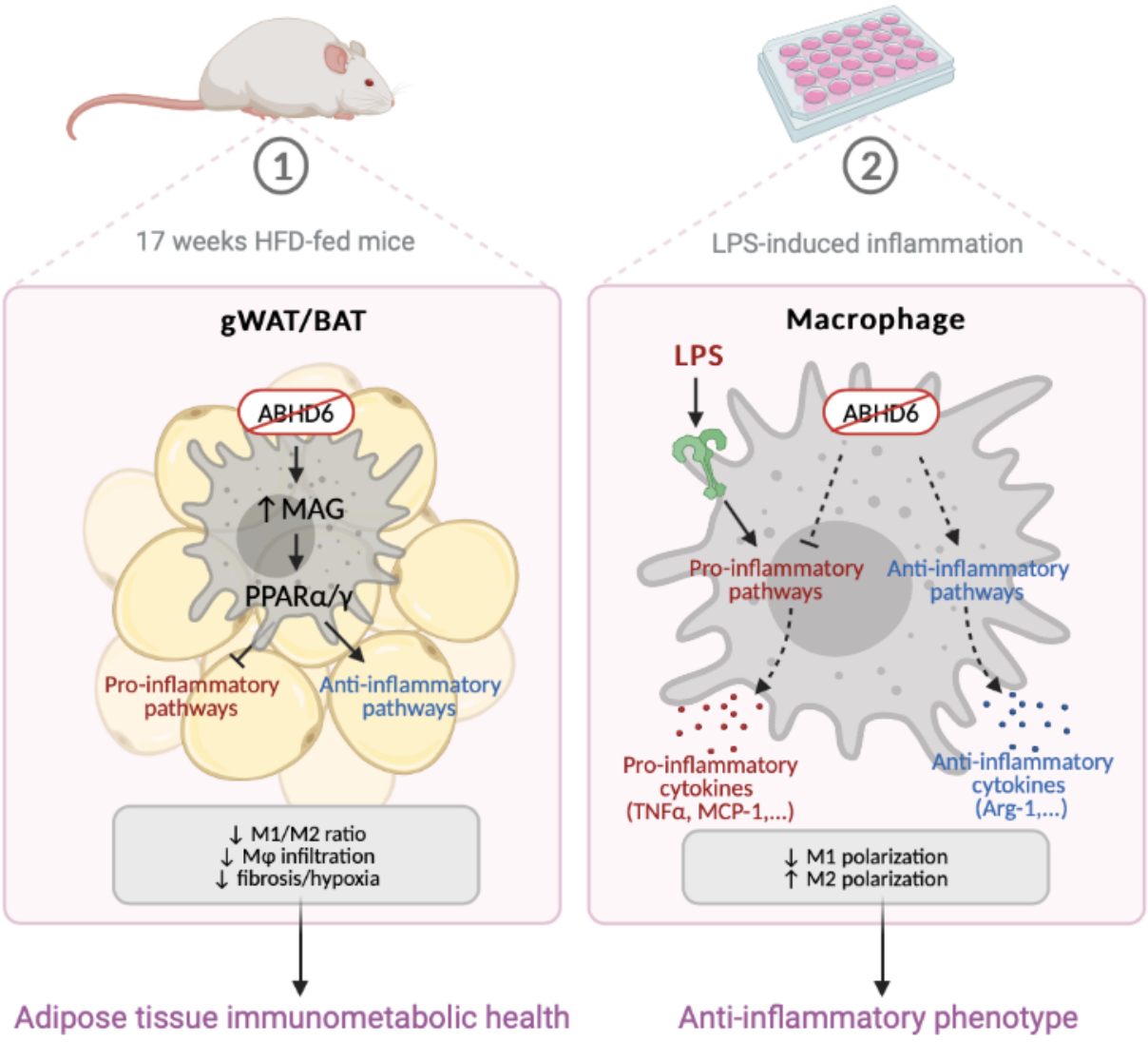

Figure 14. Schematic overview of ABHD6 suppression effects in the AT of HFD-mice and in the LPS-stimulated macrophages.

Global deletion of ABHD6 in HFD-fed mice leads to the accumulation of the of MAG in the gWAT- and BAT adipocytes, inducing PPARα/γ activation, which inhibits pro-inflammatory pathways and activates anti-inflammatory signalization. This results in the reduced M1-like macrophage population in gWAT and BAT, and contributes to enhanced AT immunometabolic health in obesity. Pharmacological inhibition of ABHD6 in macrophages stimulated with LPS induces a downregulation of the pro-inflammatory pathways, which reduces M1 polarization and the secretion of pro-inflammatory cytokines. Oppositely, ABHD6 inhibition in LPS-stimulated

macrophages activates anti-inflammatory signaling pathways, leading to polarization of macrophages towards M2-like phenotype.

4.1. The global role of ABHD6 in diet-induced chronic low-grade inflammation

ABHD6 has been shown to be upregulated in different autoimmune and inflammatory conditions. For example, high expression of ABHD6 has been observed by analyzing eQTLs (expression quantitative loci) and also mRNA levels on microarrays in the lymphoblastoid cells from a cohort of European patients with SLE, an autoimmune disease, in comparison with normal control subjects (98). ABHD6 gene expression was also found to be highly elevated in different types of cancer cells, such as U2OS cells (osteocarcinoma), PC-3 prostate cancer cells, Jurkat leukemic T-cell lymphoblast and pancreatic ductal adenocarcinoma tumors (99, 100). Also, diet-induced obesity in mice led to an increase in ABHD6 mRNA expression in the small intestine and liver (68). Thus, to address the first aim of this MSc thesis ("to assess the immunometabolic role of ABHD6 in obesity-induced AT chronic inflammation in mice"), we first examined ABHD6 expression in different adipose depots of obese and diabetic male mice. We showed that ABHD6 mRNA expression was upregulated in the gWAT, iWAT and BAT of HFD-fed mice and in the gWAT of a diabetic mice model (*db*/*db*), compared to control mice. These results, along with the previous studies mentioned above, suggest the involvement of AT ABHD6 in inflammatory and metabolic disorders.

Our research group previously showed that global deletion of ABHD6 in mice protects from diet-induced obesity and its complications (77). Here, to assess the role of ABHD6 in diet-induced AT inflammation, we also used WB-ABHD6-KO and WT mice and fed them with 60% HFD for 17 weeks. It is known that female mice are largely protected from diet-induced inflammation (93, 101). More precisely, a study reported that despite showing a similar weight after HFD treatment, male but not female mice developed a low-grade inflammation associated with an increased population of inflammatory macrophages in intra-abdominal adipose tissues and a decreased

population of anti-inflammatory Treg cell (93). Actually, estrogens have been shown to be protective against metabolic diseases and glucose-intolerance. In fact, treatment of hyperinsulinemic female *ob/ob* mice with 17β-estradiol resulted in improved glucose metabolism and more insulin sensitivity (102, 103). Thus, we only used male mice in this study. We now report in this thesis that HFD-fed WB-ABHD6-KO male mice display a protection against diet-induced obesity shown by reduced body weight, fed glycemia, and iWAT, liver, spleen and heart weights, as well as a reduced TG accumulation in both liver and spleen, compared to HFD-fed WT mice, as well as changes in inflammatory parameters that will be discussed in detail below.

During the development of obesity, the long-term positive energy balance progressively leads to AT hypoxia, inflammation and fibrosis (50-52). We previously demonstrated that global deletion of ABHD6 protects against systemic inflammation by reducing pro-inflammatory cytokine levels and enhancing anti-inflammatory cytokines in the plasma of HFD-fed mice (77). Here we have shown that the pro-inflammatory, fibrotic and hypoxic profiles of the three ATs were improved in the KO mice compared to the control group. The VC WAT isolated from HFD-KO mice exhibited reduced mRNA expression of the pro-inflammatory cytokines (*Mcp1* and *Cd11c*), fibrosis (*Col5a1*) and hypoxic (*Hif1a*) markers, associated with an upregulation of the *Arg1* anti-inflammatory M2-macrophage marker. Also, the pro-inflammatory marker *Tnfa* and the fibrosis marker *Col1a1* were only reduced in the BAT of HFD-KO mice but not in the WATs compared to HFD-WT. Overall, the results of this thesis indicate that ABHD6 deletion is associated with an improvement of AT microenvironment health, which is more pronounced in gWAT and BAT, rather than iWAT. Actually, these results go along with our previous study showing an enhanced BAT function and WAT browning in HFD-KO mice, associated with smaller adipocytes in WATs and smaller adipocytes with less lipid deposition in BAT (77). Additional studies will focus on histological analysis of ATs, such as F4/80 staining for macrophage population and Masson's staining for fibrosis.

Moreover, flow cytometry analysis showed that the number of M1 macrophages was reduced only in the SVF from gWAT and BAT depots, but not iWAT SVF from HFD-fed ABHD6-KO mice compared to WT mice. Also, the anti-inflammatory M2-macrophage population was significantly enhanced in the SVF from brown adipose depot. These results concur with the previous findings

of this thesis showing a more pronounced effect of ABHD6 deletion in reducing inflammation in the gWAT of HFD-fed mice compared to iWAT, suggesting fat depot-specific roles of ABHD6 (77, 92). Consistently, there are differences in the adipokine secretion of VC versus SC ATs, which may influence AT-resident macrophage metabolism and phenotype. For example, VC AT secretes more resistin, which is considered a pro-inflammatory adipokine and worsen insulin resistance and inflammation (35). Oppositely, SC fat produces more adiponectin which promotes M2 polarization and anti-inflammatory cytokine release (4, 18, 35). Thus, these data indicate that ABHD6 might have distinct roles in the different adipose depots under inflammatory conditions. Additional studies are needed to clarify the underlying mechanisms governing different functions of adipose ABHD6 in the context of obesity.

4.2. The role of ABHD6 in macrophage polarization

HFD feeding in mice induces a metabolic endotoxemia or enhanced level of plasma LPS. Endogenous LPS was found to be produced by gut Gram-negative bacteria which reach the circulation by crossing the intestinal barrier (104). Likewise, chronic ingestion of LPS diluted in oil by ND-fed mice led to an increased in plasma LPS levels and body weight, as well as liver insulin resistance, fasted hyperinsulinemia, and AT inflammation, similar to HFD-fed mice (104). As TLR ligands and LPS are strong inducers of the classical activation of macrophages towards M1-phenotype, here in addition to chronic diet-induced inflammation, we have also studied macrophage activation/ polarization under acute inflammation by LPS.

In LPS-stimulated macrophage cell lines and primary peritoneal macrophages, suppression of ABHD6 leads to protection from acute LPS-induced inflammatory response, shown by the downregulation of pro-inflammatory M1-markers, and reduced secretion of proinflammatory cytokines. Interestingly, ABHD6 suppression in LPS-stimulated macrophages results in the upregulation of the anti-inflammatory M2 marker *Arg-1*, suggesting that ABHD6 suppression could switch LPS-induced M1 polarization toward an anti-inflammatory M2-polarization. Nonetheless, ABHD6 inhibition did not promote additional effect to the M2-polarization induced

in IL-4-stimulated macrophages, shown by an unchanged expression of *Arg1* compared to controlled cells treated with IL-4.

Besides our present results, an *in vitro* study previously showed that ABHD6 pharmacological inhibition in macrophage cell lines and primary macrophages, using WWL70, reduces LPS-induced macrophage activation to an M1-phenotype. More precisely, they associated this effect of ABHD6 suppression to the conversion of 2-AG (an ABHD6 substrate) into prostaglandin-D2-glycerol ester (PGD2-G) by COX-2 (89). However, considering that WWL70 is not highly selective for ABHD6 (105), in the present study, we used a next-generation ABHD6 inhibitor, KT203, which has been proved to have a greater potency, selectivity and activity (73). Overall, our results showed that ABHD6 suppression in LPS-treated macrophages favored the alternative activation toward an M2-phenotype over the M1-polarization. And these data demonstrate the involvement of ABHD6 in macrophage polarization, only under LPS-induced inflammation. Future studies will be conducted to clarify the mechanisms and actors involved in the pro-inflammatory role of ABHD6 under LPS-induced inflammation.

4.3. Conclusion

Following the alarming raise of obesity prevalence over the last decades, it became crucial to determine the many actors and mechanisms involved in the physiopathology of obesity in order to find new therapeutic strategies. AT, and its complex cell network and endocrine function, contributes considerably to the obesity-associated AT inflammatory responses, which influence partly the activation and polarization of macrophages in the AT microenvironment (6, 11, 12, 25). Thus, providing insights on the mechanisms and actors involved in AT-resident macrophage polarization towards an anti-inflammatory M2 phenotype might help to develop new strategies to treat obesity and its complications.

This study identified a novel pro-inflammatory role of ABHD6 under HFD- and LPS-induced inflammation conditions. Indeed, we have shown the upregulation of WAT ABHD6 expression in the obese and diabetic mice. We also demonstrated the involvement of ABHD6 in the

immunometabolic response to obesity-induced AT inflammation in the VC white and brown adipose depots. The improved AT immunometabolic health in gWAT and BAT of HFD-ABHD6-KO mice, was revealed by reduced M1 macrophage population, M1/M2 ratio, as well as fibrosis and hypoxia markers. Moreover, we observed an increased anti-inflammatory M2-macrophage population in the SVF of the BAT, isolated from HFD-ABHD6-KO mice compared to HFD-fed WT mice. Finally, our acute inflammation studies revealed a novel effect of ABHD6 inhibition/suppression in switching LPS-induced M1 polarization toward an anti-inflammatory M2 phenotype in macrophages. These results provide an insight into the role of ABHD6 in AT immunometabolic pathways in obesity condition, and suggest ABHD6 as a therapeutic target for inflammation and obesity-related complications.

4.4. Perspectives

This study proposed a new role for ABHD6 in the AT inflammatory responses to HFD and LPS treatments. However, the cellular and molecular pathways involved in this pro-inflammatory function of ABHD6 in AT-resident macrophages under inflammatory conditions remains unstudied. Several cellular mechanisms could be considered for further research on the subject.

Depending on the tissue or cellular localization, ABHD6 hydrolyzes different lipidic substrates, mostly MAGs, and control various functions (62). Previous study from our lab demonstrated that ABHD6 deletion led to the accumulation of 1-MAG in white and brown ATs, and 1-MAG was responsible for the activation of PPARα and γ by direct binding (77). Moreover, antagonism of PPARα was shown to reverse ABHD6-KO beneficial metabolic effects in mice and adipose browning and thermogenic program (77). Actually, PPARα regulates lipid and lipoprotein metabolism in several tissues, while PPARγ is known as the master regulator of lipogenesis and adipocyte differentiation (84-86). Additionally, PPARγ activation also triggers AT macrophage polarization towards an M2-phenotype (6, 25). Finally, PPARs antagonize AP-1 and NF-κB, thereby inhibit the transcription of pro-inflammatory genes. Therefore for future steps, it could be important to look into signalling molecules involved in PPARs pathways in the SVF of ATs from

HFD-fed ABHD6-KO and HFD-WT mice, in LPS-stimulated macrophage cell-lines (treated with KT203), and upon ABHD6 overexpression in macrophages and adipocytes cell lines.

In addition, 2-AG, the first ABHD6 substrate found in the CNS, activates CB1 and 2 receptors, and the products of 2-AG hydrolysis might also activates PPARα and γ. First, CB2 receptor is highly expressed in immune cells such as macrophages, however its activation by 2-AG showed anti- and pro-inflammatory effects depending on the experimental conditions and cell lines used (62, 80-82). Thus, the absence of ABHD6 could induce the accumulation of 2-AG in certain cells/conditions and the following effects are unknown. Second, 2-AG hydrolysis by ABHD6 or COX-2 generates arachidonic acid, a precursor of prostaglandins, which are well known to be involved in inflammatory responses (88). However, an *in vitro* study showed that, upon ABHD6 inhibition in LPS-stimulated macrophages, 2-AG is converted by COX-2 to PGD2-G instead, which had a more anti-inflammatory effect (89). This study also demonstrated that ABHD6 inhibition and 2-AG effects were independent of cannabinoid receptors, as well as PPARs, in LPS-stimulated macrophages (89). Now, it would be important to include lipidomics analysis of the SVF of ATs from HFD-fed ABHD6-KO and HFD-WT mice, and in macrophage cell lines stimulated with LPS, in order to understand the underlying mechanisms involved in the diet-induced inflammation responses.

Another point to address is the differences observed between the adipose fat depots in the responses to HFD-induced inflammation. We point out that the differences in the adipokine secretion of the different ATs can influence the polarization of the AT-resident macrophages and cytokine release (6, 25). This could start by simple measurements of leptin, adiponectin and resistin and maybe other adipokines secretion from the gWAT, iWAT and BAT from HFD-KO and -WT. Then, we should confirm the differences in inflammatory and fibrotic profile with histologic studies, such as F4/80 staining for macrophage population, and Masson's staining for fibrosis.

Lastly, to further reveal the metabolic switch from an M1-phenotype towards an M2-phenotype in LPS-treated macrophages, we could investigate their glucose and lipid metabolism in addition to M1 and M2 markers. It is known that M1 and M2 macrophages have different metabolic phenotypes. M1 macrophages express high levels of nitric oxide (NO) synthase, which synthesize

NO from arginine, and NO levels are easily measurable using Griess reagent (106). Also, M1 mostly use aerobic glycolysis to fuel the TCA cycle and produce lipids, HIF-1α and prostaglandins (106). Again, substrates from glycolysis can be detected and quantify, such as lactate release upon LPS-stimulation. M2 macrophages express Arg-1, which synthesize arginine, and will be used to produce precursors of collagen for tissue repair (106). They also use FA oxidation and FFA to fuel the mitochondrial oxidative phosphorylation, which is triggered by PPARγ activation (106). Glucose and fat metabolism from macrophages can be measured by cellular oxygen consumption rates (OCR) and extracellular acidification rates (ECAR) using a Seahorse extracellular flux analyser.

Nonetheless, there are some limitations in this study that need to be noted. First, only male mice were used. Even though female mice are largely protected against diet-induced inflammation, we could have confirmed this phenotype in our mice model. Second, as HFD elevates fibrosis, hypoxia and inflammation in adipose tissue, and ND-fed mice exhibited no or limited phenotype in this study (**Figure 10**), we continued only on HFD-fed mice and we did not show ND-fed mice in all the figures (50-52). Also, it is difficult to analyze macrophage-specific gene expression in the adipose tissue because of the limited number of cells and the heterogeneity of the cells found in the whole adipose depots. Notably, flow cytometry is the most precise method to examine ATM composition (107). Thus, we first showed the inflammatory profile of the whole adipose tissue (**Figure 11**), and then, we confirmed our phenotype by looking into better markers using flow cytometry in isolated SVF (**Figure 12**).

To conclude, this study proposed ABHD6 as a new therapeutic target for obesity associated inflammatory disorders. The protective effect of ABHD6 suppression against HFD-induced AT inflammation results from the switch from M1-polarization to an anti-inflammatory M2 polarization of AT-resident macrophages. The cellular and molecular pathways involved in the regulation of macrophage polarization by ABHD6 under inflammatory conditions still need to be studied. Some studies revealed that targeting macrophage polarization toward M2 polarization had significant effects to counteract metabolic diseases, such as obesity and atherosclerosis (108-112). Thus, providing insights on the mechanisms and actors involved in AT-resident macrophage

polarization towards an anti-inflammatory M2 phenotype upon ABHD6 inhibition might help to develop new strategies to treat obesity and its complications.

Références bibliographiques

All the figures were generated using Biorender.com.

1. Organization WH. Global Health Observatory data 2017 [Available from: https://www.who.int/gho/ncd/risk_factors/overweight/en/.
2. Quail DF, Dannenberg AJ. The obese adipose tissue microenvironment in cancer development and progression. Nature Reviews Endocrinology. 2019;15(3):139-54.
3. Reilly SM, Saltiel AR. Adapting to obesity with adipose tissue inflammation. Nature Reviews Endocrinology. 2017;13(11):633-43.
4. Brestoff JR, Artis D. Immune regulation of metabolic homeostasis in health and disease. Cell. 2015;161(1):146-60.
5. Jin C, Henao-Mejia J, Flavell RA. Innate immune receptors: key regulators of metabolic disease progression. Cell Metab. 2013;17(6):873-82.
6. Lumeng CN, Saltiel AR. Inflammatory links between obesity and metabolic disease. J Clin Invest. 2011;121(6):2111-7.
7. Osborn O, Olefsky JM. The cellular and signaling networks linking the immune system and metabolism in disease. Nat Med. 2012;18(3):363-74.
8. Public Health Agency of Canada CIfHI. Obesity in Canada: A joint report from the public health agency of Canada and the Canadian institute for health information. Public Health Agency of Canada Ottawa; 2011.
9. Bartelt A, Heeren J. Adipose tissue browning and metabolic health. Nature Reviews Endocrinology. 2014;10(1):24-36.
10. Chait A, den Hartigh LJ. Adipose Tissue Distribution, Inflammation and Its Metabolic Consequences, Including Diabetes and Cardiovascular Disease. Front Cardiovasc Med. 2020;7:22.
11. Ghaben AL, Scherer PE. Adipogenesis and metabolic health. Nature Reviews Molecular Cell Biology. 2019;20(4):242-58.
12. Fasshauer M, Blüher M. Adipokines in health and disease. Trends in Pharmacological Sciences. 2015;36(7):461-70.
13. Bartness TJ, Liu Y, Shrestha YB, Ryu V. Neural innervation of white adipose tissue and the control of lipolysis. Front Neuroendocrinol. 2014;35(4):473-93.
14. Bartness TJ, Vaughan CH, Song CK. Sympathetic and sensory innervation of brown adipose tissue. Int J Obes (Lond). 2010;34 Suppl 1(0 1):S36-S42.
15. Lo KA, Sun L. Turning WAT into BAT: a review on regulators controlling the browning of white adipocytes. Bioscience reports. 2013;33(5).
16. Wang W, Kissig M, Rajakumari S, Huang L, Lim HW, Won KJ, et al. Ebf2 is a selective marker of brown and beige adipogenic precursor cells. Proc Natl Acad Sci U S A. 2014;111(40):14466-71.
17. Shao M, Ishibashi J, Kusminski CM, Wang QA, Hepler C, Vishvanath L, et al. Zfp423 Maintains White Adipocyte Identity through Suppression of the Beige Cell Thermogenic Gene Program. Cell Metab. 2016;23(6):1167-84.
18. Kahn CR, Wang G, Lee KY. Altered adipose tissue and adipocyte function in the pathogenesis of metabolic syndrome. J Clin Invest. 2019;129(10):3990-4000.

19. Tran TT, Kahn CR. Transplantation of adipose tissue and stem cells: role in metabolism and disease. Nat Rev Endocrinol. 2010;6(4):195-213.
20. Lu J, Zhao J, Meng H, Zhang X. Adipose tissue-resident immune cells in obesity and type 2 diabetes. Frontiers in immunology. 2019;10:1173.
21. Viola A, Munari F, Sánchez-Rodríguez R, Scolaro T, Castegna A. The metabolic signature of macrophage responses. Frontiers in immunology. 2019;10.
22. Odegaard JI, Chawla A. Alternative macrophage activation and metabolism. Annual Review of Pathology: Mechanisms of Disease. 2011;6:275-97.
23. Liu R, Nikolajczyk BS. Tissue immune cells fuel obesity-associated inflammation in adipose tissue and beyond. Frontiers in immunology. 2019;10.
24. dos Anjos Cassado A. F4/80 as a Major Macrophage Marker: The Case of the Peritoneum and Spleen. In: Kloc M, editor. Macrophages: Origin, Functions and Biointervention. Cham: Springer International Publishing; 2017. p. 161-79.
25. Murray PJ, Wynn TA. Protective and pathogenic functions of macrophage subsets. Nature reviews immunology. 2011;11(11):723-37.
26. Winer DA, Winer S, Shen L, Wadia PP, Yantha J, Paltser G, et al. B cells promote insulin resistance through modulation of T cells and production of pathogenic IgG antibodies. Nat Med. 2011;17(5):610-7.
27. Crewe C, An YA, Scherer PE. The ominous triad of adipose tissue dysfunction: inflammation, fibrosis, and impaired angiogenesis. The Journal of clinical investigation. 2017;127(1):74-82.
28. Ma X, Lee P, Chisholm DJ, James DE. Control of Adipocyte Differentiation in Different Fat Depots; Implications for Pathophysiology or Therapy. Front Endocrinol (Lausanne). 2015;6(1).
29. Bunnell BA, Flaat M, Gagliardi C, Patel B, Ripoll C. Adipose-derived stem cells: isolation, expansion and differentiation. Methods. 2008;45(2):115-20.
30. Moreno-Navarrete JM, Fernández-Real JM. Adipocyte differentiation. Adipose tissue biology: Springer; 2017. p. 69-90.
31. Lee RA, Harris CA, Wang J-C. Glucocorticoid Receptor and Adipocyte Biology. Nucl Receptor Res. 2018;5:101373.
32. Warbrick I, Rabkin SW. Hypoxia-inducible factor 1-alpha (HIF-1α) as a factor mediating the relationship between obesity and heart failure with preserved ejection fraction. Obesity Reviews. 2019;20(5):701-12.
33. Pereira SS, Alvarez-Leite JI. Adipokines: biological functions and metabolically healthy obese profile. Journal of Receptor, Ligand and Channel Research. 2014;7:15-25.
34. Mancuso P, Bouchard B. The Impact of Aging on Adipose Function and Adipokine Synthesis. Front Endocrinol (Lausanne). 2019;10:137-.
35. Scheja L, Heeren J. The endocrine function of adipose tissues in health and cardiometabolic disease. Nature Reviews Endocrinology. 2019;15(9):507-24.
36. Guilherme A, Henriques F, Bedard AH, Czech MP. Molecular pathways linking adipose innervation to insulin action in obesity and diabetes mellitus. Nature reviews Endocrinology. 2019;15(4):207-25.
37. Flier JS, Maratos-Flier E. Leptin's Physiologic Role: Does the Emperor of Energy Balance Have No Clothes? Cell Metabolism. 2017;26(1):24-6.

38. Ahima RS, Prabakaran D, Mantzoros C, Qu D, Lowell B, Maratos-Flier E, et al. Role of leptin in the neuroendocrine response to fasting. Nature. 1996;382(6588):250-2.
39. Larabee CM, Neely OC, Domingos AI. Obesity: a neuroimmunometabolic perspective. Nature Reviews Endocrinology. 2019:1-14.
40. Moraes-Vieira PM, Yore MM, Dwyer PM, Syed I, Aryal P, Kahn BB. RBP4 activates antigen-presenting cells, leading to adipose tissue inflammation and systemic insulin resistance. Cell metabolism. 2014;19(3):512-26.
41. Kang K, Reilly SM, Karabacak V, Gangl MR, Fitzgerald K, Hatano B, et al. Adipocyte-derived Th2 cytokines and myeloid PPARdelta regulate macrophage polarization and insulin sensitivity. Cell Metab. 2008;7(6):485-95.
42. Lee M-W, Lee M, Oh K-J. Adipose Tissue-Derived Signatures for Obesity and Type 2 Diabetes: Adipokines, Batokines and MicroRNAs. J Clin Med. 2019;8(6):854.
43. Shimizu I, Aprahamian T, Kikuchi R, Shimizu A, Papanicolaou KN, MacLauchlan S, et al. Vascular rarefaction mediates whitening of brown fat in obesity. J Clin Invest. 2014;124(5):2099-112.
44. Burýsek L, Houstek J. beta-Adrenergic stimulation of interleukin-1alpha and interleukin-6 expression in mouse brown adipocytes. FEBS Lett. 1997;411(1):83-6.
45. Qing H, Desrouleaux R, Israni-Winger K, Mineur YS, Fogelman N, Zhang C, et al. Origin and function of stress-induced IL-6 in murine models. Cell. 2020;182(2):372-87. e14.
46. Burýšek L, Houštěk J. β-Adrenergic stimulation of interleukin-1α and interleukin-6 expression in mouse brown adipocytes. FEBS letters. 1997;411(1):83-6.
47. Villarroya J, Cereijo R, Villarroya F. An endocrine role for brown adipose tissue? American Journal of Physiology-Endocrinology and Metabolism. 2013;305(5):E567-E72.
48. Poher A-L, Altirriba J, Veyrat-Durebex C, Rohner-Jeanrenaud F. Brown adipose tissue activity as a target for the treatment of obesity/insulin resistance. Frontiers in Physiology. 2015;6(4).
49. Appleton SL, Seaborn CJ, Visvanathan R, Hill CL, Gill TK, Taylor AW, et al. Diabetes and cardiovascular disease outcomes in the metabolically healthy obese phenotype: a cohort study. Diabetes Care. 2013;36(8):2388-94.
50. Hoffstedt J, Arner E, Wahrenberg H, Andersson DP, Qvisth V, Löfgren P, et al. Regional impact of adipose tissue morphology on the metabolic profile in morbid obesity. Diabetologia. 2010;53(12):2496-503.
51. Klöting N, Blüher M. Adipocyte dysfunction, inflammation and metabolic syndrome. Reviews in Endocrine and Metabolic Disorders. 2014;15(4):277-87.
52. Shao M, Vishvanath L, Busbuso NC, Hepler C, Shan B, Sharma AX, et al. De novo adipocyte differentiation from Pdgfrβ+ preadipocytes protects against pathologic visceral adipose expansion in obesity. Nature Communications. 2018;9(1):890.
53. Jin C, Flavell RA. Innate sensors of pathogen and stress: Linking inflammation to obesity. Journal of Allergy and Clinical Immunology. 2013;132(2):287-94.
54. Fitzgibbons TP, Kogan S, Aouadi M, Hendricks GM, Straubhaar J, Czech MP. Similarity of mouse perivascular and brown adipose tissues and their resistance to diet-induced inflammation. Am J Physiol Heart Circ Physiol. 2011;301(4):H1425-H37.

55. Dowal L, Parameswaran P, Phat S, Akella S, Majumdar ID, Ranjan J, et al. Intrinsic Properties of Brown and White Adipocytes Have Differential Effects on Macrophage Inflammatory Responses. Mediators of Inflammation. 2017;2017:9067049.
56. Omran F, Christian M. Inflammatory Signaling and Brown Fat Activity. Front Endocrinol (Lausanne). 2020;11(156).
57. Cai D, Yuan M, Frantz DF, Melendez PA, Hansen L, Lee J, et al. Local and systemic insulin resistance resulting from hepatic activation of IKK-beta and NF-kappaB. Nature medicine. 2005;11(2):183-90.
58. Saghizadeh M, Ong JM, Garvey WT, Henry RR, Kern PA. The expression of TNF alpha by human muscle. Relationship to insulin resistance. The Journal of clinical investigation. 1996;97(4):1111-6.
59. Bendtzen K, Mandrup-Poulsen T, Nerup J, Nielsen JH, Dinarello CA, Svenson M. Cytotoxicity of human pI 7 interleukin-1 for pancreatic islets of Langerhans. Science. 1986;232(4757):1545.
60. Zhang X, Zhang G, Zhang H, Karin M, Bai H, Cai D. Hypothalamic IKKbeta/NF-kappaB and ER stress link overnutrition to energy imbalance and obesity. Cell. 2008;135(1):61-73.
61. Prentki M, Madiraju SRM. Glycerolipid Metabolism and Signaling in Health and Disease. Endocrine Reviews. 2008;29(6):647-76.
62. Poursharifi P, Madiraju SRM, Prentki M. Monoacylglycerol signalling and ABHD6 in health and disease. Diabetes, Obesity and Metabolism. 2017;19:76-89.
63. Atawia RT, Bunch KL, Toque HA, Caldwell RB, Caldwell RW. Mechanisms of obesity-induced metabolic and vascular dysfunctions. Front Biosci (Landmark Ed). 2019;24:890-934.
64. Hafidi ME, Buelna-Chontal M, Sánchez-Muñoz F, Carbó R. Adipogenesis: A Necessary but Harmful Strategy. International journal of molecular sciences. 2019;20(15):3657.
65. Song Z, Xiaoli AM, Yang F. Regulation and Metabolic Significance of De Novo Lipogenesis in Adipose Tissues. Nutrients. 2018;10(10).
66. Blankman JL, Simon GM, Cravatt BF. A comprehensive profile of brain enzymes that hydrolyze the endocannabinoid 2-arachidonoylglycerol. Chem Biol. 2007;14(12):1347-56.
67. Zhao S, Mugabo Y, Iglesias J, Xie L, Delghingaro-Augusto V, Lussier R, et al. α/β-Hydrolase domain-6-accessible monoacylglycerol controls glucose-stimulated insulin secretion. Cell Metab. 2014;19(6):993-1007.
68. Thomas G, Betters JL, Lord CC, Brown AL, Marshall S, Ferguson D, et al. The serine hydrolase ABHD6 Is a critical regulator of the metabolic syndrome. Cell Rep. 2013;5(2):508-20.
69. Marrs WR, Blankman JL, Horne EA, Thomazeau A, Lin YH, Coy J, et al. The serine hydrolase ABHD6 controls the accumulation and efficacy of 2-AG at cannabinoid receptors. Nat Neurosci. 2010;13(8):951-7.
70. Zhong P, Pan B, Gao X-p, Blankman JL, Cravatt BF, Liu Q-s. Genetic deletion of monoacylglycerol lipase alters endocannabinoid-mediated retrograde synaptic depression in the cerebellum. J Physiol. 2011;589(Pt 20):4847-55.
71. Taschler U, Radner FP, Heier C, Schreiber R, Schweiger M, Schoiswohl G, et al. Monoglyceride lipase deficiency in mice impairs lipolysis and attenuates diet-induced insulin resistance. J Biol Chem. 2011;286(20):17467-77.
72. Li W, Blankman JL, Cravatt BF. A Functional Proteomic Strategy to Discover Inhibitors for Uncharacterized Hydrolases. Journal of the American Chemical Society. 2007;129(31):9594-5.

73. Hsu KL, Tsuboi K, Chang JW, Whitby LR, Speers AE, Pugh H, et al. Discovery and optimization of piperidyl-1,2,3-triazole ureas as potent, selective, and in vivo-active inhibitors of α/β-hydrolase domain containing 6 (ABHD6). J Med Chem. 2013;56(21):8270-9.
74. Baggelaar MP, den Dulk H, Florea BI, Fazio D, Bernabò N, Raspa M, et al. ABHD2 Inhibitor Identified by Activity-Based Protein Profiling Reduces Acrosome Reaction. ACS Chemical Biology. 2019;14(10):2295-304.
75. Zimmermann R, Strauss JG, Haemmerle G, Schoiswohl G, Birner-Gruenberger R, Riederer M, et al. Fat mobilization in adipose tissue is promoted by adipose triglyceride lipase. Science. 2004;306(5700):1383-6.
76. Bisogno T, Howell F, Williams G, Minassi A, Cascio MG, Ligresti A, et al. Cloning of the first sn1-DAG lipases points to the spatial and temporal regulation of endocannabinoid signaling in the brain. J Cell Biol. 2003;163(3):463-8.
77. Zhao S, Mugabo Y, Ballentine G, Attane C, Iglesias J, Poursharifi P, et al. α/β-Hydrolase Domain 6 Deletion Induces Adipose Browning and Prevents Obesity and Type 2 Diabetes. Cell Rep. 2016;14(12):2872-88.
78. Sugiura T, Kondo S, Sukagawa A, Nakane S, Shinoda A, Itoh K, et al. 2-Arachidonoylglycerol: a possible endogenous cannabinoid receptor ligand in brain. Biochem Biophys Res Commun. 1995;215(1):89-97.
79. Spigelman I. Therapeutic targeting of peripheral cannabinoid receptors in inflammatory and neuropathic pain states. Translational Pain Research: From Mouse to Man. 2010:99-138.
80. Pertwee RG. Pharmacological actions of cannabinoids. Handb Exp Pharmacol. 2005(168):1-51.
81. Sugiura T. Physiological roles of 2-arachidonoylglycerol, an endogenous cannabinoid receptor ligand. BioFactors (Oxford, England). 2009;35:88-97.
82. Kishimoto S, Kobayashi Y, Oka S, Gokoh M, Waku K, Sugiura T. 2-Arachidonoylglycerol, an endogenous cannabinoid receptor ligand, induces accelerated production of chemokines in HL-60 cells. J Biochem. 2004;135(4):517-24.
83. Lee S-A, Yang KJZ, Brun P-J, Silvaroli JA, Yuen JJ, Shmarakov I, et al. Retinol-binding protein 2 (RBP2) binds monoacylglycerols and modulates gut endocrine signaling and body weight. Science Advances. 2020;6(11):eaay8937.
84. Evans RM, Barish GD, Wang YX. PPARs and the complex journey to obesity. Nat Med. 2004;10(4):355-61.
85. Bishop-Bailey D, Swales KE. The Role of PPARs in the Endothelium: Implications for Cancer Therapy. PPAR Res. 2008;2008:904251-.
86. Anghel SI, Wahli W. Fat poetry: a kingdom for PPAR gamma. Cell Res. 2007;17(6):486-511.
87. Hubler MJ, Kennedy AJ. Role of lipids in the metabolism and activation of immune cells. J Nutr Biochem. 2016;34:1-7.
88. Ricciotti E, FitzGerald GA. Prostaglandins and inflammation. Arterioscler Thromb Vasc Biol. 2011;31(5):986-1000.
89. Alhouayek M, Masquelier J, Cani PD, Lambert DM, Muccioli GG. Implication of the anti-inflammatory bioactive lipid prostaglandin D2-glycerol ester in the control of macrophage activation and inflammation by ABHD6. Proceedings of the National Academy of Sciences. 2013;110(43):17558.

90. Wen J, Ribeiro R, Tanaka M, Zhang Y. Activation of CB2 receptor is required for the therapeutic effect of ABHD6 inhibition in experimental autoimmune encephalomyelitis. Neuropharmacology. 2015;99:196-209.
91. Tchantchou F, Zhang Y. Selective Inhibition of Alpha/Beta-Hydrolase Domain 6 Attenuates Neurodegeneration, Alleviates Blood Brain Barrier Breakdown, and Improves Functional Recovery in a Mouse Model of Traumatic Brain Injury. Journal of Neurotrauma. 2012;30(7):565-79.
92. Poursharifi P, Attané C, Mugabo Y, Al-Mass A, Ghosh A, Schmitt C, et al. Adipose ABHD6 regulates tolerance to cold and thermogenic programs. JCI Insight. 2020;5(24):e140294.
93. Pettersson US, Waldén TB, Carlsson P-O, Jansson L, Phillipson M. Female mice are protected against high-fat diet induced metabolic syndrome and increase the regulatory T cell population in adipose tissue. PloS one. 2012;7(9):e46057.
94. Skarnes WC, Rosen B, West AP, Koutsourakis M, Bushell W, Iyer V, et al. A conditional knockout resource for the genome-wide study of mouse gene function. Nature. 2011;474(7351):337-42.
95. Cho KW, Morris DL, Lumeng CN. Flow cytometry analyses of adipose tissue macrophages. Methods Enzymol. 2014;537:297-314.
96. Zhang X, Goncalves R, Mosser DM. The isolation and characterization of murine macrophages. Curr Protoc Immunol. 2008;Chapter 14:Unit-14.1.
97. Ruiz-Ojeda FJ, Méndez-Gutiérrez A, Aguilera CM, Plaza-Díaz J. Extracellular Matrix Remodeling of Adipose Tissue in Obesity and Metabolic Diseases. International journal of molecular sciences. 2019;20(19):4888.
98. Oparina NY, Delgado-Vega AM, Martinez-Bueno M, Magro-Checa C, Fernández C, Castro RO, et al. PXK locus in systemic lupus erythematosus: fine mapping and functional analysis reveals novel susceptibility gene ABHD6. Annals of the rheumatic diseases. 2015;74(3):e14-e.
99. Li F, Fei X, Xu J, Ji C. An unannotated α/β hydrolase superfamily member, ABHD6 differentially expressed among cancer cell lines. Molecular biology reports. 2009;36(4):691-6.
100. Grüner BM, Schulze CJ, Yang D, Ogasawara D, Dix MM, Rogers ZN, et al. An in vivo multiplexed small-molecule screening platform. Nature methods. 2016;13(10):883-9.
101. Nickelson KJ, Stromsdorfer KL, Pickering RT, Liu T-W, Ortinau LC, Keating AF, et al. A comparison of inflammatory and oxidative stress markers in adipose tissue from weight-matched obese male and female mice. Experimental diabetes research. 2012;2012.
102. Louet JF, LeMay C, Mauvais-Jarvis F. Antidiabetic actions of estrogen: insight from human and genetic mouse models. Curr Atheroscler Rep. 2004;6(3):180-5.
103. Lundholm L, Bryzgalova G, Gao H, Portwood N, Fält S, Berndt KD, et al. The estrogen receptor {alpha}-selective agonist propyl pyrazole triol improves glucose tolerance in ob/ob mice; potential molecular mechanisms. J Endocrinol. 2008;199(2):X1.
104. Cani PD, Amar J, Iglesias MA, Poggi M, Knauf C, Bastelica D, et al. Metabolic endotoxemia initiates obesity and insulin resistance. Diabetes. 2007;56(7):1761-72.
105. Tanaka M, Moran S, Wen J, Affram K, Chen T, Symes AJ, et al. WWL70 attenuates PGE(2) production derived from 2-arachidonoylglycerol in microglia by ABHD6-independent mechanism. J Neuroinflammation. 2017;14(1):7.
106. Batista-Gonzalez A, Vidal R, Criollo A, Carreño LJ. New Insights on the Role of Lipid Metabolism in the Metabolic Reprogramming of Macrophages. Frontiers in Immunology. 2020;10(2993).

107. Cho KW, Morris DL, Lumeng CN. Flow cytometry analyses of adipose tissue macrophages. Methods in enzymology. 2014;537:297-314.
108. Johnson AR, Qin Y, Cozzo AJ, Freemerman AJ, Huang MJ, Zhao L, et al. Metabolic reprogramming through fatty acid transport protein 1 (FATP1) regulates macrophage inflammatory potential and adipose inflammation. Molecular metabolism. 2016;5(7):506-26.
109. Boutens L, Hooiveld GJ, Dhingra S, Cramer RA, Netea MG, Stienstra R. Unique metabolic activation of adipose tissue macrophages in obesity promotes inflammatory responses. Diabetologia. 2018;61(4):942-53.
110. Yang X, Li Y, Li Y, Ren X, Zhang X, Hu D, et al. Oxidative stress-mediated atherosclerosis: mechanisms and therapies. Frontiers in physiology. 2017;8:600.
111. Teupser D, Kretzschmar D, Tennert C, Burkhardt R, Wilfert W, Fengler Dr, et al. Effect of macrophage overexpression of murine liver X receptor-α (LXR-α) on atherosclerosis in LDL-receptor deficient mice. Arteriosclerosis, thrombosis, and vascular biology. 2008;28(11):2009-15.
112. Calkin AC, Tontonoz P. Liver x receptor signaling pathways and atherosclerosis. Arteriosclerosis, thrombosis, and vascular biology. 2010;30(8):1513-8.

Annexes

Appendix A. Mice normal diet composition

2018

ENVIGO

Teklad Global 18% Protein Rodent Diet

Product Description- 2018 is a fixed formula, non-autoclavable diet manufactured with high quality ingredients and designed to support gestation, lactation, and growth of rodents. 2018 does not contain alfalfa, thus lowering the occurrence of natural phytoestrogens. Typical isoflavone concentrations (daidzein + genistein aglycone equivalents) range from 150 to 250 mg/kg. Exclusion of alfalfa reduces chlorophyll, improving optical imaging clarity. Absence of animal protein and fish meal minimizes the presence of nitrosamines. **Also available certified (2018C) and irradiated (2918). For autoclavable diet, refer to 2018S (Sterilizable) or 2018SX (Extruded & Sterilizable).**

Ingredients (in descending order of inclusion)- Ground wheat, ground corn, wheat middlings, dehulled soybean meal, corn gluten meal, soybean oil, calcium carbonate, dicalcium phosphate, brewers dried yeast, iodized salt, L-lysine, DL-methionine, choline chloride, kaolin, magnesium oxide, vitamin E acetate, menadione sodium bisulfite complex (source of vitamin K activity), manganous oxide, ferrous sulfate, zinc oxide, niacin, calcium pantothenate, copper sulfate, pyridoxine hydrochloride, riboflavin, thiamin mononitrate, vitamin A acetate, calcium iodate, vitamin B_{12} supplement, folic acid, biotin, vitamin D_3 supplement, cobalt carbonate.

Standard Product Form: ***Pellet***

Macronutrients		
Crude Protein	%	18.6
Fat (ether extract) [a]	%	6.2
Carbohydrate (available) [b]	%	44.2
Crude Fiber	%	3.5
Neutral Detergent Fiber [c]	%	14.7
Ash	%	5.3
Energy Density [d]	kcal/g (kJ/g)	3.1 (13.0)
Calories from Protein	%	24
Calories from Fat	%	18
Calories from Carbohydrate	%	58
Minerals		
Calcium	%	1.0
Phosphorus	%	0.7
Non-Phytate Phosphorus	%	0.4
Sodium	%	0.2
Potassium	%	0.6
Chloride	%	0.4
Magnesium	%	0.2
Zinc	mg/kg	70
Manganese	mg/kg	100
Copper	mg/kg	15
Iodine	mg/kg	6
Iron	mg/kg	200
Selenium	mg/kg	0.23
Amino Acids		
Aspartic Acid	%	1.4
Glutamic Acid	%	3.4
Alanine	%	1.1
Glycine	%	0.8
Threonine	%	0.7
Proline	%	1.6
Serine	%	1.1
Leucine	%	1.8
Isoleucine	%	0.8
Valine	%	0.9
Phenylalanine	%	1.0
Tyrosine	%	0.6
Methionine	%	0.4
Cystine	%	0.3
Lysine	%	0.9
Histidine	%	0.4
Arginine	%	1.0
Tryptophan	%	0.2

Vitamins		
Vitamin A [e, f]	IU/g	15.0
Vitamin D_3 [e, g]	IU/g	1.5
Vitamin E	IU/kg	110
Vitamin K_3 (menadione)	mg/kg	50
Vitamin B_1 (thiamin)	mg/kg	17
Vitamin B_2 (riboflavin)	mg/kg	15
Niacin (nicotinic acid)	mg/kg	70
Vitamin B_6 (pyridoxine)	mg/kg	18
Pantothenic Acid	mg/kg	33
Vitamin B_{12} (cyanocobalamin)	mg/kg	0.08
Biotin	mg/kg	0.40
Folate	mg/kg	4
Choline	mg/kg	1200
Fatty Acids		
C16:0 Palmitic	%	0.7
C18:0 Stearic	%	0.2
C18:1ω9 Oleic	%	1.2
C18:2ω6 Linoleic	%	3.1
C18:3ω3 Linolenic	%	0.3
Total Saturated	%	0.9
Total Monounsaturated	%	1.3
Total Polyunsaturated	%	3.4
Other		
Cholesterol	mg/kg	--

[a] Ether extract is used to measure fat in pelleted diets, while an acid hydrolysis method is required to recover fat in extruded diets. Compared to ether extract, the fat value for acid hydrolysis will be approximately 1% point higher.

[b] Carbohydrate (available) is calculated by subtracting neutral detergent fiber from total carbohydrates.

[c] Neutral detergent fiber is an estimate of insoluble fiber, including cellulose, hemicellulose, and lignin. Crude fiber methodology underestimates total fiber.

[d] Energy density is a calculated estimate of *metabolizable energy* based on the Atwater factors assigning 4 kcal/g to protein, 9 kcal/g to fat, and 4 kcal/g to available carbohydrate.

[e] Indicates added amount but does not account for contribution from other ingredients.

[f] 1 IU vitamin A = 0.3 µg retinol

[g] 1 IU vitamin D = 25 ng cholecalciferol

For nutrients not listed, insufficient data is available to quantify.

Nutrient data represent the best information available, calculated from published values and direct analytical testing of raw materials and finished product. Nutrient values may vary due to the natural variations in the ingredients, analysis, and effects of processing.

Teklad Diets are designed and manufactured for research purposes only.

0915

Teklad Diets + Madison WI + envigo.com + tekladinfo@envigo.com + (800) 483-5523

Appendix B. Mice HFD composition

RESEARCH DIETS INC.

Caloric Information **Physiological Fuel Values**

Protein:	**20**% kcal
Fat:	**60**% kcal
Carbohydrate:	**20**% kcal
Energy Density:	**5.21** kcal/g

D12492

Rodent Diet With 60 kcal% Fat

Intended species: Rodent (Rat/Mouse)
Color: Blue
Irradiated: D12492i

Talk with one of our nutrition scientists about your next project. Let us formulate the experimental and matching control diets to meet your specific study needs.

Formulation

Class description	Ingredient	Grams
Protein	Casein, Lactic, 30 Mesh	200.00 g
Protein	Cystine, L	3.00 g
Carbohydrate	Lodex 10	125.00 g
Carbohydrate	Sucrose, Fine Granulated	72.80 g
Fiber	Solka Floc, FCC200	50.00 g
Fat	Lard	245.00 g
Fat	Soybean Oil, USP	25.00 g
Mineral	S10026B	50.00 g
Vitamin	Choline Bitartrate	2.00 g
Vitamin	V10001C	1.00 g
Dye	Dye, Blue FD&C #1, Alum. Lake 35-42%	0.05 g
	Total:	773.85 g

20 Jules Lane New Brunswick, NJ 08901 USA Tel: 732.247.2390 Fax: 732.247.2340 info@researchdiets.com

Appendix C. Antibodies

Antibodies	Dilutions	Source	Reference
Anti-ABHD6 (D3C8N)	1/1000	Cell Signaling Technology	97573
Anti-β-actin (AC-15)	1/10000	Sigma-Aldrich	A5441
Anti-CD11b BB515	1/500	BD Biosciences	564455
Anti-CD11c BV421	1/200	BD Biosciences	565451
Anti-CD301 Alexa647	1/50	Biorad	MCA2392A647T
Anti-F4/80 BV785	1/200	Biolegend	123141
Anti-CD45.2 PE- Cy™7	1/200	BD Biosciences	560696
Anti-CD16/CD32 (Fc-block)	1/100	Tonbo Biosciences	70-0161-M001

Appendix D. Primers sequences

Gene		Sequence
m18s	Forward	CTG AGA AAC GGC TAG CAC ATC
	Reverse	GGC CTC GAA AGA GTC CTG TAT
mAbhd6	Forward	AGA CCA GGT GCT TGA TGT
	Reverse	CTC TCC ATC ACT ACC GAA T
mArg1	Forward	AGA CCA CAG TCT GGC AGT TG
	Reverse	CCA CCC AAA TGA CAC ATA GG
mMcp1	Forward	GCAGTTAACGCCCCACTCA
	Reverse	CCCAGCCTACTCATTGGGATCA
mTnfa	Forward	CCAAGGCGCCACATCTCCCT
	Reverse	GCTTTCTGTGCTCATGGTGT
mCd11c	Forward	GTGCTGAGTTCGGACACAGT
	Reverse	AGAGGCCACCTATTTGGTTAGT
mMrc1	Forward	CTCTGTTCAGCTATTGGACGC
	Reverse	CGGAATTTCTGGGATTCAGCTTC
mCol1a1	Forward	AGATGATGGGGAAGCTGGCAA
	Reverse	AAGCCTCGGTGTCCCTTCATT
mCol5a1	Forward	TGTCATGTTTGGCTCCCGGAT
	Reverse	AGTCATAGGCAGCTCGGTTGT
mHif1a	Forward	GGGGAGGACGATGAACATCAA
	Reverse	GGGTGGTTTCTTGTACCCACA